Cogent Engineering

ISSN: 2331-1916 (Online) Journal homepage: www.tandfonline.com/journals/oaen20

Demand response for efficient power generation in smart grids using hyper–local weather prediction

Faraz Shaikh, Hasan Ali Khattak, Hasan Sohaib Alavi, Haleem Farman & Moustafa M. Nasralla

To cite this article: Faraz Shaikh, Hasan Ali Khattak, Hasan Sohaib Alavi, Haleem Farman & Moustafa M. Nasralla (2025) Demand response for efficient power generation in smart grids using hyper–local weather prediction, Cogent Engineering, 12:1, 2555341, DOI: 10.1080/23311916.2025.2555341

To link to this article: https://doi.org/10.1080/23311916.2025.2555341

COGENT ENGINEERING
2025, VOL. 12, NO. 1, 2555341
https://doi.org/10.1080/23311916.2025.2555341

ELECTRICAL AND ELECTRONIC ENGINEERING | RESEARCH ARTICLE
OPEN ACCESS
Check for updates

Demand response for efficient power generation in smart grids using hyper–local weather prediction

Faraz Shaikh[a,b], Hasan Ali Khattak[a,c], Hasan Sohaib Alavi[d], Haleem Farman[e] and Moustafa M. Nasralla[e]

[a]School of Electrical Engineering and Computer Science (SEECS), National University of Sciences and Technology (NUST), Islamabad, Pakistan; [b]Department of Engineering, University of Perugia, Perugia, Umbria, Italy; [c]School of Computer, Data & Mathematical Sciences, Western Sydney University, Sydney, NSW, Australia; [d]Beyond Engineering NL BV, Harderwijk Gelderland, Netherlands; [e]Smart Systems Engineering Lab, Communications and Networks Engineering Department, College of Engineering, Prince Sultan University, Riyadh, Saudi Arabia

ABSTRACT

Optimizing power generation is crucial in the evolving smart grid and urban ecosystem landscape. Efficient energy use is vital in today's tech-driven world, with smart grids leading the way in managing energy consumption and distribution. Given the link between climate and energy use, integrating weather data is now essential. This research presents a method combining demand response in smart grids with hyperlocal weather predictions using machine learning to enhance power generation forecasts. Five models—SARIMAX, Prophet, XGBoost, LSTM, and Holt–Winters are trained on the smart grid and weather data, including precipitation, humidity, temperature, and cloud cover. Extensive feature engineering, such as lag terms and cyclic encoding, improved accuracy. SARIMAX outperformed others with an MAE of 3.54 and an *R*-squared of 0.97, while the hybrid model, combining SARIMAX, Prophet, and Holt–Winters, achieved an *R*-squared of 0.96. The hybrid model's dynamic recalibration improved accuracy with new data. A real-time dashboard is also developed, offering dynamic, user-specific forecasting insights. This research enhances smart grid management by integrating machine learning and demand response for more efficient energy use.

ARTICLE HISTORY
Received 16 September 2024
Revised 11 February 2025
Accepted 16 March 2025

KEYWORDS
Hyperlocal weather prediction; machine learning; smart grid; short-term load forecasting; time series forecasting

SUBJECTS
Renewable Energy; Technology; Computer Science (General); Information & Communication Technology (ICT); Software Engineering & Systems Development; Systems & Computer Architecture

1. Introduction

Electricity is a critical component of our everyday lives, industries, and technological breakthroughs in the modern world. Electricity generation is mainly concerned with transforming various kinds of energy into electrical power, such as fossil fuels, nuclear, hydro, wind, or solar (Rajagopalan, 2022). This produced energy is delivered across great distances via a network of high-voltage transmission lines. When it arrives at its destination, the voltage is lowered by substations and delivered to individual customers via a network of distribution lines, which includes residential, commercial, and industrial users. Traditionally, electricity generation has depended on centralized power facilities that use resources such as coal, natural gas, or nuclear reactions (Sathyaraj & Sankardoss, 2024). These factories are deliberately positioned for safety and environmental concerns, generally near energy sources or away from inhabited areas. In its conventional form, the grid has been the backbone of electricity delivery, ensuring plant power reaches consumers efficiently. However, this traditional grid is limited to unidirectional flow and communication, primarily focusing on delivering electricity without active demand management or real-time adjustments based on consumption patterns.

CONTACT Faraz Shaikh faraz@dottorandi.unipg.it National University of Sciences and Technology, NUST, SEECS, Islamabad, 44500, Islamabad, Pakistan, Department of Engineering, University of Perugia, Via G. Duranti 93, Perugia, 06125, Umbria, Italy.

A smart grid (SG) is an improved electrical grid system integrating digital communication technology to improve power distribution efficiency, reliability, and sustainability. Unlike traditional grids, SGs provide bidirectional communication between electricity producers and consumers, allowing real-time monitoring and automatic response to changing demand and supply situations (Amin, 2025). This dynamic interaction enables the integration of distributed energy resources (DERs), such as solar and wind power, improving electricity generation, distribution, and consumption. SGs may use advanced data analytics and machine learning (ML) to forecast demand patterns, control energy flow, and ensure grid stability even as the energy environment grows more complicated and decentralized.

An SG operation depends on accurate power demand forecasts and renewable energy production. The development of SGs is a meaningful change for the power sector, bringing many advantages and new challenges. The future of energy management and consumption is anticipated to be significantly shaped by SGs as research and development continue. However, the unpredictable nature of renewable energy sources (RESs) and the wide range of user behaviors make the prediction process problematic (Xia et al., 2021). For SG operators and solar energy suppliers, accurate forecasting of energy generation, especially solar power, is essential. Due to its considerable reliance on weather factors, renewable power needs accurate forecasts to guarantee power continuity and make suitable preparations for energy dispatch and storage (Carrera & Kim, 2020). The switch to SG, however, is not without its complications. Predicting energy demand and supply correctly in an SG is becoming more innovative and interconnected. Without adequate planning, a rapid decline in renewable energy generation might cause blackouts and unstable system conditions (Jamii et al., 2022).

Weather has always significantly influenced energy demand, especially regarding RESs such as solar and wind. The production predictability of these renewable sources becomes increasingly important as our globe turns to them. RESs are subject to the whims of nature, as opposed to conventional energy sources, which can be managed and changed in response to demand. For instance, there might be variations in the amount of energy produced if the sun does not shine and the wind does not blow (Gowtham et al., 2023). On the other hand, heavy rains, storms, and high temperatures have substantially disrupted energy production and delivery. In many countries, these conditions can result in total blackouts or decreased energy output, primarily if the system relies highly on renewable sources such as solar or wind (Carreras et al., 2021). These factors require precise weather predictions for RESs to provide regular electricity availability and grid stability.

While helpful, traditional weather forecast systems sometimes lack the granularity and precision required to handle sudden and localized changes in meteorological conditions, which can significantly impact renewable energy generation. Large-scale weather models often produce projections for large areas, which are insufficient for controlling unpredictability at the micro-scale where RESs function (Zhang et al., 2024). As a result, these models may fail to forecast localized weather events that might have severe consequences for energy output, such as unexpected cloud cover over a solar farm or isolated wind gusts impacting wind turbines.

This gap in standard forecasting approaches emphasizes the need for hyperlocal weather predictions. Hyperlocal forecasting provides a solution by generating high-resolution data that is both temporally and spatially precise. With this degree of precision, energy operators can more accurately forecast and respond to weather-related changes in energy output. Integrating hyperlocal weather prediction into SG operations can be crucial for maximizing power output, especially when utilizing RESs such as solar and wind. Hyperlocal weather prediction gives accurate, localized data on climatic factors, including solar irradiance, wind speed, and temperature, which directly influence RESs' efficiency and output (Venter et al., 2020). Accurate forecasting of these factors enables better control of renewable energy's intrinsic unpredictability and fluctuation, improving SG dependability and stability. Recent advances in digital twin technology and ML models have proven the capacity to accurately anticipate renewable energy generation by modeling different weather conditions in real-time (Wang et al., 2023). This ability is critical to facilitating the smooth integration of RESs into the grid, maximizing energy dispatch, and decreasing operating costs. While this strategy is unique in its application to SGs, it is inspired by approaches employed in other electrical systems, such as dynamic line rating (DLR). DLR has successfully used hyperlocal meteorological data to improve the accuracy of power transmission projections (Manninen et al., 2024). Although the context changes, this highlights the efficacy of combining extensive environmental data with ML models tailored to SG management's unique requirements and problems.

1.1. Problem statement

This paper addresses the critical issue of precise and dependable short-term power generation and demand predictions in SGs. RESs' unpredictability and shifting consumer demand affect the grid's balance and efficiency, making this a critical challenge for the SG's stability and optimization.

Traditional weather forecasting methods using hyperlocal weather predictions, such as those addressed in recent studies, primarily use physics-based numerical weather prediction (NWP) models. While these models produce reliable forecasts, they are limited by medium spatial resolutions and high computing demands, making them less suitable for real-time applications in SGs that require rapid and targeted responses. These restrictions impede the capacity to properly manage energy resources, particularly in scenarios involving dispersed microgrids (Zaidan et al., 2024). On the other hand, recent advances in forecasting systems, such as using vast sensor infrastructures and edge computing, have sought to provide real-time hyper–local weather predictions. However, these systems may confront issues in processing the massive volumes of data collected, assuring forecast accuracy and dependability, and doing so efficiently enough to incorporate into SG operations (Adkins et al., 2023).

To address these gaps, this work focuses on enhancing short-term load forecasting (STLF) in SGs using hyper–local meteorological data with a forecasting horizon of up to 48 hours. Our technique hybridizes sophisticated time series models such as SARIMAX, Prophet, and Holt–Winters exponential smoothing, giving appropriate weights to each model to improve prediction accuracy while retaining computing efficiency. This technique overcomes geographical and temporal resolution limits and improves data processing for real-time applications.

The issue's relevance lies in its influence on SGs' operational efficiency. Accurate forecasting is critical for optimal resource allocation, grid stability, and lowering operating costs, primarily as modern SGs rely more on RESs and dynamic demand response systems.

1.2. Motivation

In many developing nations, including Pakistan, frequent blackouts and power outages have become a substantial barrier to economic progress and daily living. Blackouts are caused by a variety of conditions, including an uneven energy supply–demand ratio, outdated transmission and distribution infrastructure, and inefficient grid management. One key factor is the insufficient integration of RESs, such as solar and wind power, which are intermittent and pose problems to grid stability. Furthermore, fluctuating fuel prices and unbalanced fuel imports have an impact on thermal power generation (World Bank, 2020), inflating the problem. Pakistan's energy consumption is quickly increasing due to increasing population and urbanization. It continues to rely heavily on fossil fuel-based power generation, which is both economically and ecologically unsustainable. Power plants running on imported fuels, such as natural gas or oil, are sensitive to supply chain interruptions, resulting in deficits. Additional reasons contributing to frequent load shedding and unscheduled outages include poor grid maintenance, a lack of infrastructure investment, and energy theft (Jamil, 2018).

In this context, SGs provide a possible option to reduce blackouts by integrating distributed renewable energy supplies, enhancing grid management, and increasing operational efficiency. However, these SGs confront the challenges of maintaining dependable power generation and distribution, given the uncertain RESs and varying customer demands. This study focuses on tackling these issues by using sophisticated forecasting approaches that combine hyperlocal weather data with demand response mechanisms. This study attempts to deliver more reliable forecasting solutions for real-time SG operations by merging these models into a hybrid framework and employing dynamic recalibration approaches.

1.3. Contributions of the research

1. Development of a novel forecasting framework that combines machine learning (ML) algorithms with hyperlocal meteorological data and demand response mechanisms, resulting in short-term load forecasting (STLF) in SG. This unique combination enhances prediction accuracy by dynamically adapting to fluctuating weather conditions and energy demand patterns.

2. Comprehensive evaluation and benchmarking of individual forecasting models (SARIMAX, Prophet, and Holt–Winters) within the context of SG applications. This work gives deep insights into the relative effectiveness of various models, highlighting their distinct strengths and limits in estimating energy use, which has not been thoroughly investigated in previous studies.
3. Introduction of a novel hybrid model approach that incorporates real-time dynamic re-calibration. This technique modifies the weighting of individual model components based on their real-time performance, resulting in adaptive, context-sensitive prediction.
4. Development of a real-time adaptive forecasting dashboard that allows user-specific customization and flexibility for varying prediction periods. This practical tool is intended to improve operational decision-making in SGs by offering quick, accurate, and highly customized forecasting choices.
5. Exploration of the practical and long-term effects of integrating hyperlocal weather data into SG operations. The model paves the way for more effective energy distribution and management, notably through greater integration of renewable energy sources, leading to less energy waste and increased grid sustainability.

1.4. Key highlights

- Demand Response systems optimize SG Power Generation Efficiency.
- User-adaptive dashboards enable customized power forecast visualizations.
- Integration of hyperlocal weather data significantly enhances prediction accuracy.
- The SARIMAX model stands out with an R-squared score of 0.97
- The Hybrid Time series model achieves an *R*-squared score of 0.96.

The rest of the paper is organized as follows: Section 1 gives the readers a thorough background on SG and its applications, along with basic definitions. Section 2 presents a detailed literature review and a comparative analysis of the state of the art. Section 3 briefly explains collection, pre-processing, and feature engineering techniques used on the data. Section 4 represents a baseline method for evaluating demand response in a SG for a specific locality. A detailed explanation of the experimental analysis is given in Section 5, the results of which are discussed in detail in Section 6. Following this, the parameter sensitivity and ablation study are given in Section 7. Further, we present the contributions of this work along with possible future directions in Section 8. The last Section 9 gives the concluding remarks for the paper.

2. Related work

Over the past decade, electrical systems have transformed. Traditional power networks have undergone significant adjustments to fit the dynamic nature of contemporary energy demands and the integration of RESs. These grids were built initially for a one-way flow of electricity from centralized production sources to users. There was a rush in research on the grid integration of RESs in the early 2010s. FitzPatrick and Wollman (2010) emphasized the significance of developing a road map for SG interoperability standards, highlighting the challenges of incorporating various energy sources. The groundwork for comprehending the complexity of contemporary power systems was laid.

Demand-side management (DSM) is a comprehensive method that includes several tactics for optimizing consumer energy usage, such as increasing energy efficiency, regulating load, and responding to dynamic price signals. The authors of Bakare et al. (2023) divided DSM operations into three categories: demand response, distributed energy resources (DER), and energy efficiency (EE), with each confronting issues such as integrating intermittent RESs, correct load classification, and the use of dynamic pricing. A crucial component of DSM, particularly within SGs, is Demand Response Management (DRM). DRM is the ability of end users to adjust their electrical use in response to variations in the cost of electricity over time or between various energy sources (Ahmed et al., 2024). The significance of DRM in SGs became apparent as the decade went on. With the growing integration of RESs whose production might be irregular and unexpected, DRM systems played a crucial role in ensuring grid stability (Adnan et al., 2023).

Further, the issues RESs encounter, notably their reliance on environmental conditions, have become a research focus in recent decades. While smart meters enabled real-time demand prediction, it was realized that there was an urgent need for precise models to anticipate the power provided by renewable sources (Arumugham et al., 2023). These models were critical for ensuring grid stability, practical scheduling, and energy management. For example, if a model anticipated that renewable energy would be lost, the SG would need to transition smoothly to conventional energy sources to guarantee that the generated power matched the predicted demand.

Using artificial intelligence (AI) in SGs has opened new research opportunities. AI-based DSM technique by Ullah et al., (2022) evaluated in various case studies shows reductions in operational costs of up to 3.5% and emissions of up to 14.5%. More enhancements utilizing the Multi-Objective Genetic Algorithm (MOGA) result in significant cost and emission savings yet the approach's limitations stem from the uncertainty of wind energy forecast using Monte Carlo simulations, which may affect scheduling precision. Further, to improve demand responsiveness in SGs, the Pre-Attention Mechanism and Convolutional Neural Network-based Multivariate Load Prediction model are used, achieving a Mean Absolute Percentage Error (MAPE) ranging from 9 to 11% (He et al., 2023). These algorithms ensure effective power generation and give actionable performance insights on the SG system. However, the model's generalizability to different datasets is restricted, and its computational cost may pose issues for real-time applications.

Hyperlocal weather forecasts are localized ones that usually target small geographic regions, such as individual city blocks or neighborhoods (Li & Sharma, 2024). Hyperlocal forecasts have given granular data with high geographical and temporal precision, unlike standard weather forecasts that provide broad information for more prominent regions. The importance of hyperlocal weather prediction in SGs has been highlighted by Adkins et al., (2023) in urban air mobility, Balážová et al. (2024) in drone operations, and Zaidan et al. (2024) in renewable energy forecasting known as *IrMaSet*. The *IrMaSet* reduced forecast errors significantly with reported reductions in prediction errors, i.e., 353,143 kWh underestimation and a 359,968 kWh overestimation in solar energy generation. Improved forecasting can reduce CO_2 emissions of 17.55 tonnes at a maximum annually (claimed by authors). Yet, the system's reliance on low-cost sensors might cause data quality challenges, and its computational and maintenance requirements may have operational complexity.

Temperature, wind speed, and humidity influence RESs, changing the quantity of power they generate. *NowCasting* developed by Krishna et al. (2018) used for short-term wind power prediction using autoregression models provides forecasts ranging from 10 minutes to 6 hours in advance, achieving a normalized mean absolute error (MAE) of 2.11% to 14.25%. But the accuracy of these hyperlocal predictions is largely reliant on the quality and reliability of input data, which can be influenced by sensor imperfections and environmental variation. Furthermore, the model's effectiveness may suffer in places with limited sensor coverage or high geographical and temporal variability in wind patterns. Advanced ML and deep learning (DL) algorithms, including Gaussian Process Regression (GPR), have been developed by Li and Sharma (2024) to increase prediction accuracy, achieving an *R*-squared score (R^2) of up to 0.95. However, the prediction reported an MAE of about 1.7 °C in temperature predictions, with MAE surpassing 2.5 °C in locations with fewer sensors. Sensor drift and local environmental conditions can cause further variances. Ibrahim et al. (2022) explored ML techniques for STLF in SGs, predicting demand from one hour to 24 hours ahead, emphasizing the importance of meteorological factors like temperature. Key predictors included the previous week's and last day's same-hour loads. The DL regression model achieved an R^2 score of 0.93 and MAPE of 2.9%, while the Ada-Boost model had an R^2 score of 0.75 and MAPE of 5.70%. But, due to the number of hidden layers used, the model took an average of 20 minutes to train, and the GRU multi-step model performed badly, particularly with long input sequences and the vanishing gradient problem demonstrating that multi-step prediction remains a challenging area in the field.

Traditional statistical approaches such as Autoregressive Moving Average (ARMA), Autoregressive Integrated Moving Average (ARIMA), and exponential smoothing often fail to capture complex nonlinear relationships in STLF (Das & Chakrabarti, 2021). In contrast, ML methods have shown superior performance. A study on India's Wholesale Price Index (WPI) using a Multi-Layer Perceptron (MLP) model demonstrated better accuracy compared to traditional methods, with MAPE improvements ranging from

56% to 92% in various simulations (Das & Chakrabarti, 2021). However, of the 72 WPIs investigated, 52 did not match the model, leaving their performance unexplored and raising concerns about the model's application to datasets with no discernible patterns. The analysis was restricted to 25 WPIs with discernible non-linear patterns, reducing the total assessment. Similarly, Tarmanini et al. (2023) compared ARIMA and Artificial Neural Network (ANN) methods for STLF in Ireland, finding that ANN outperformed ARIMA with a MAPE of 1.80% compared to 2.61%. On the other hand, DL approaches have also shown promising results in resolving the constraints of statistical-based models. They can simulate sophisticated non-linear mappings between inputs and outputs, detect hidden patterns in large datasets, and provide scalability. The model's performance may vary depending on the household's specific consumption habits, which are impacted by external factors such as weather and vacations, emphasizing the need for more comprehensive models.

In SGs, dynamic pricing methods, such as, Time of Use (ToU), Real-Time Pricing (RTP), and Critical Peak Pricing (CPP) are also employed to regulate energy usage and facilitate the integration of RESs. While RTP helps RES integration and lowers peak demand, communication and measurement requirements complicate consumer planning. ToU permits good consumer planning and is easy to deploy, however, it has minimal influence on supply/demand and RES integration. To solve these difficulties, CPP minimizes peak demand and displays fixed pricing levels, however, it has limited usage hours and does not enable RES integration. Using these pricing methods, Salazar et al. (2023) developed a reinforcement learning-based pricing and incentive method for demand response in SGs based on short-term and long-term Q-Learning algorithms. The proposed approach reduced peak demand by an average of 8% and the peak-to-average ratio by 6–22%, resulting in an overall cost reduction of around 4%, with a maximum decrease of 12%. Whereas, the complexity of using both short-term and long-term Q-Learning methods may hinder real-time implementation, which necessitates large computer resources. Also, the model's performance can be impacted by a variety of customer actions, which may result in unsatisfactory outcomes if not properly accounted for.

A prosumer is an individual or an organization that produces and consumes energy often using RESs such as solar or wind. Prosumer-centric SG systems leveraging the engagement of both producers and consumers in energy management and exchange are becoming increasingly popular. Patrizi et al. (2022) developed a self-sustaining prosumer-centric SG model that uses contract theory to optimize interactions between prosumers and grid operators, assuring a balance of energy supply and demand while being economically sustainable. This model emphasizes the relevance of dynamic pricing mechanisms and DERs, allowing prosumers to actively participate in grid operations by exchanging excess energy and altering usage in response to real-time price signals. While this strategy improves local grid management, the proposed study builds on previous work by concentrating on forecasting approaches combined with hyperlocal meteorological data to maximize energy distribution and system stability. The use of advanced ML models (e.g., LSTM, SARIMAX, XGBoost, and hybrid models) addresses the challenge of accurate load and renewable energy forecasting, resulting in improved grid efficiency and stability while remaining consistent with existing research.

In summary, integrating RESs and advanced ML techniques has significantly enhanced SGs' efficiency and responsiveness. While traditional statistical methods have limitations, modern ML and DL approaches offer superior prediction accuracy. The integration of hyperlocal weather forecasts further supports grid stability and energy management. Current forecasting models often don't account for hyperlocal weather variations, leading to inefficiencies in energy management and grid stability. Continued research in hybrid models and advanced algorithms is essential for addressing remaining challenges and optimizing SG performance.

3. Data collection and pre-processing

Time series data for SG battery storage has been sourced from IEEE Dataport[1]. The data is from Taiwan and contains 76966 data records involving 28 variables related to Energy storage, i.e., power factor, frequency, current, and voltage for each phase in a three-phase power storage system, apparent and real Power, and others. The data spans from 01 September to 30 September 2022. The sampling frequency of the data is 30 seconds. Meanwhile, the weather data has been sourced separately from Open-Meteo[2]. The weather data is hyperlocal, and the location coordinates are used only to have weather data for the specific locality for September 2022. The weather data contains the variables, i.e., temperature, relative humidity, apparent temperature, precipitation, cloud cover, and wind speed. The sampling frequency of weather data is hourly.

A few preprocessing steps are taken before the analysis. For time series consistency, missing values were found in the datasets and imputed using linear interpolation. *Z* score analysis and visual examination using box plots are used to identify outliers, which were then dealt with to ensure they did not skew the results. Data normalization was done to scale the features to a standard range. Also, the two datasets are merged by using joins and balancing the data accordingly, as one dataset is sampled hourly, and the other is sampled every 30 seconds.

Some of the data pre-processing steps are discussed as follows.

3.1. Exploratory data analysis (EDA)

The first step in EDA is to examine the distribution of the data. Histograms are plotted for weather variables, i.e., temperature, relative humidity, apparent temperature, precipitation, cloud cover, and wind speed, to understand their distribution and detect any skewness or bias (Figure 1). The histograms show that most meteorological variables have a normal distribution, yet considerable skewness in precipitation and cloud cover is seen.

Similarly, histograms for grid variables, including power factor, frequency, current, voltage, and others, are generated to check for normality and distribution characteristics (Figure 2). These histograms show that while most grid parameters follow a normal distribution, there are notable power factor and frequency deviations.

Further, Tables 1 and 2 define the summary statistics of both datasets, showing the statistical metrics relative to the weather and grid data. These analyses show that weather variables, such as, temperature and humidity significantly influence renewable energy generation due to their solid correlations and observable patterns hence accurate weather predictions are crucial for reliable energy forecasting. The insights gained from EDA are important for incorporating detailed weather data and robust preprocessing methods to enhance the precision and reliability of power generation predictions.

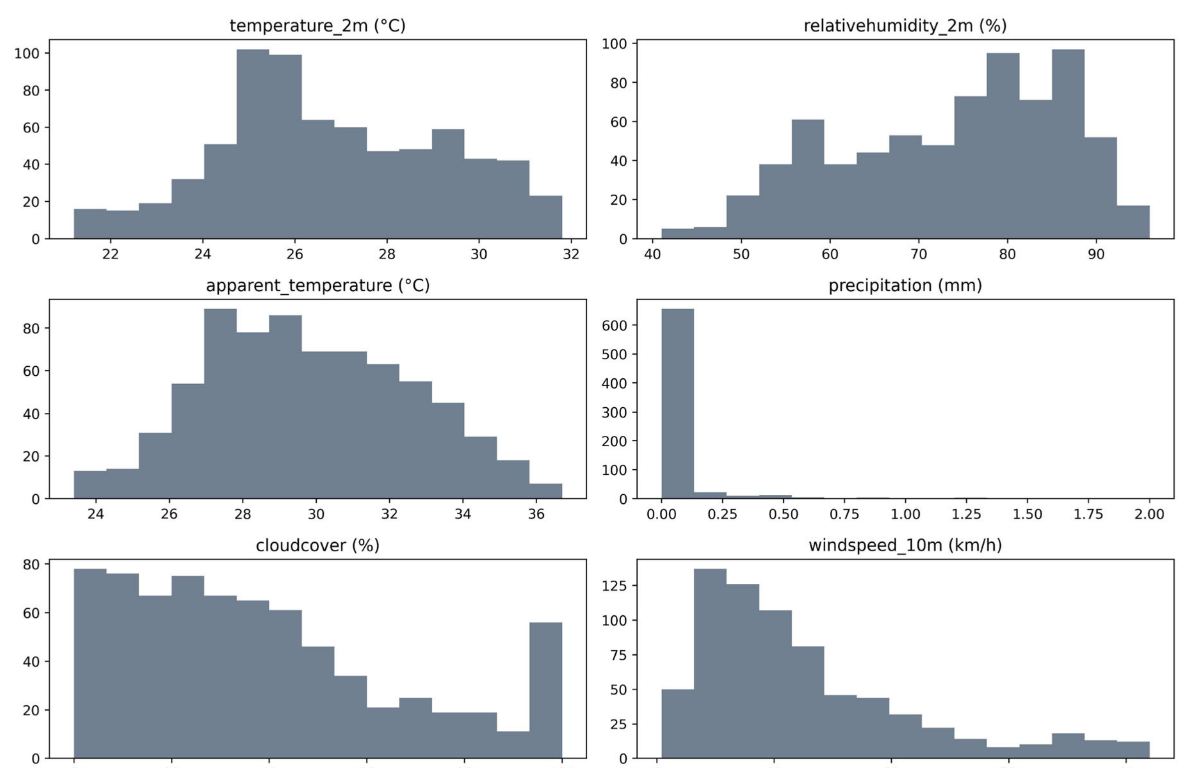

Figure 1. Histograms for weather data variables.

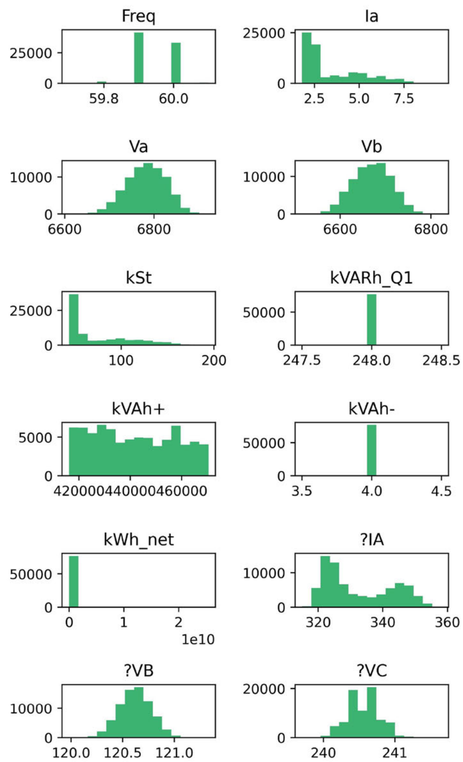

Figure 2. Histograms for grid data variables.

Table 1. Summary statistics for weather data variables.

Variable	Count	Mean	Std dev	Min	Max
Temperature (°C)	720	26.77	2.40	21.20	31.80
Relative humidity (%)	720	73.63	12.48	41.00	96.00
Apparent temperature (°C)	720	29.78	2.80	23.40	36.70
Precipitation (mm)	720	0.06	0.21	0.00	2.00
Cloud cover (%)	720	38.53	28.19	0.00	100.00
Wind speed (km/h)	720	12.59	9.26	0.40	42.00

Table 2. Summary statistics for grid data variables (kPt is the dependent variable).

Variable	Count	Mean	Std dev	Min	Max
Frequency (Hz)	76966	59.94	0.05	59.70	60.10
Ia (A)	76966	3.49	1.64	1.80	9.60
Ib (A)	76966	3.46	1.74	1.80	9.80
Ic (A)	76966	3.91	1.60	2.40	10.00
Power Factor	76966	0.79	0.12	0.55	0.99
Va (V)	76966	6782.30	43.33	6610.00	6922.00
Vb (V)	76966	6669.81	42.27	6516.00	6823.00
Vc (V)	76966	6787.31	43.79	6608.00	6945.00
kPt (kW)	76967	124.89	17324.39	26.00	4806344.00
kQt (kVAR)	76966	−33.11	2.04	−40.00	−24.00
kSt (kVA)	76966	74.43	33.27	44.00	194.00
kVARh Q1	76966	248.00	0.00	248.00	248.00
kVARh Q2	76966	0.00	0.00	0.00	0.00
kVARh Q3	76966	0.00	0.00	0.00	0.00
kVARh Q4	76966	223415.90	7076.36	211194.00	235660.00
kVAh+	76966	441499.05	15796.76	416178.00	470412.00
kVAh-	76966	4.00	0.00	4.00	4.00
kWh+	76967	661180.43	9171421.00	309786.00	2544541000.00
kWh-	76967	0.00	0.00	0.00	0.00
kWh abs	76966	330596.12	13328.15	309788.00	355400.00
kWh net	76967	661177.21	9171377.00	309784.00	2544441000.00
?IA	76966	332.53	10.47	315.00	358.15
?IB	76966	81.28	15.80	51.67	115.25
?IC	76966	205.63	14.01	185.61	241.55
?VA	76966	0.00	0.00	0.00	0.00
?VB	76966	120.62	0.15	119.98	121.33
?VC	76966	240.56	0.21	239.70	241.65

3.2. Addressing non-stationarity in time series

Hypothesis testing is a fundamental statistical technique for determining the validity of a particular hypothesis about a dataset. In time series analysis, the null hypothesis often states that the series has a unit root, implying non-stationarity and the presence of time-dependent characteristics. The alternative hypothesis is that the time series is stationary, suggesting it lacks a time-dependent structure (Pasari & Shah, 2020).

The Augmented Dickey–Fuller (ADF) test determines the presence of a unit root in a time series. Using the ADF test on the dataset, the test statistic did not fall below the critical values at the generally used confidence levels (1%, 5%, and 10%), and the p value surpassed 0.05, suggesting that the null hypothesis of a unit root could not be rejected, as shown in Figure 3.

To further investigate stationarity, rolling mean and standard deviation were used. The rolling mean MA_t at time $_t$ smoothes out short-term variations by averaging the data across a set interval n, revealing the underlying trend, and is defined as Eq. (1):

$$\mathrm{MA}_t = \frac{1}{n}\sum_{i=0}^{n-1} X_{t-i} \tag{1}$$

The rolling standard deviation SD_t measures the variability within this frame. It indicates how much the data deviates from the rolling mean over time, as shown in Eq. (2).

$$\mathrm{SD}_t = \sqrt{\frac{1}{n}\sum_{i=0}^{n-1} (X_{t-i} - \mathrm{MA}_t)^2} \tag{2}$$

As shown in Figure 3, the rolling mean varies over the month, reflecting changes in the average of the time series. Similarly, the rolling standard deviation shows changing volatility, with larger values suggesting more unpredictability in the data. Periodic peaks and troughs in the original data indicate a cyclical time series component. The fact that the rolling mean and standard deviation do not remain constant over time suggests that the time series is non-stationary, which means that its statistical properties, such as mean and variance, do not remain consistent. This result emphasizes the necessity for further feature engineering to solve the issue of non-stationarity.

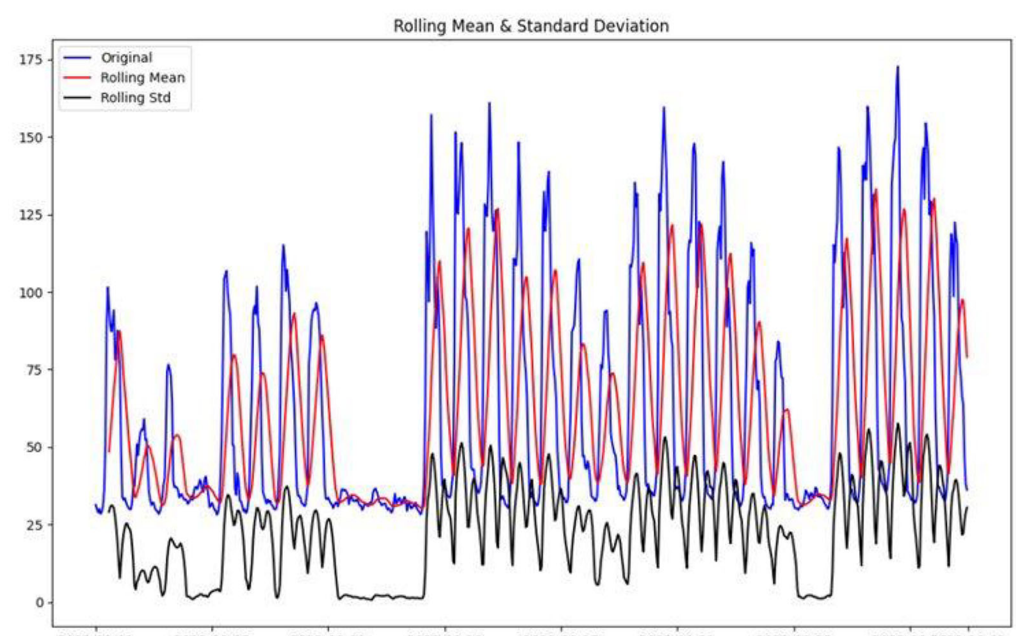


```
Results of Dickey-Fuller Test:
Test Statistic                 -2.253411
p-value                         0.187434
#Lags Used                     20.000000
Number of Observations Used   699.000000
Critical Value (1%)            -3.439740
Critical Value (5%)            -2.865684
Critical Value (10%)           -2.568977
dtype: float64
```

Figure 3. Ducky–Fuller test showing rolling mean and standard deviation.

3.3. Feature engineering

Given the non-stationarity found in the time series using the ADF test, extra feature engineering approaches were required to stabilize the statistical features of the data and increase the model's prediction accuracy. The primary goal of these strategies is to convert the time series into a format that highlights the underlying patterns and correlations while decreasing noise and guaranteeing that data is forecastable. This section describes the simple yet sophisticated feature engineering approaches, such as log transformation, lag features, and cyclic variables, leading to better forecasting of the dependent variable *kPt*.

3.3.1. Log transformation

Log transformation is used to reduce variation and heteroscedasticity (when the variance (spread) of errors or residuals in a dataset is not constant across different levels over time) in time series data. The transformation eliminates skewness and linearizes exponential growth patterns, making the data more suitable for linear modeling techniques. The log transformations performed are shown in Eqs. (3) and (4):

$$y' = \log(y + 1) \tag{3}$$

$$y'' = \log(y + 2) \tag{4}$$

where:

- y is the original value of the time series
- y' is the log-transformed value.

Adding *1* ensures that the transformation can be applied even to zero values. For example, if $kPt = 1000$ kW at time t, then the transformed value would be $\log(1000 + 1) \approx 3.0004$ making the series more stationary by reducing the variability over time.

3.3.2. Lag features

Lag features introduce previous values of the dependent variable, *kPt*, as predictors for the current value. This method allows the model to capture the data's temporal dependencies and autoregressive patterns. By adding these lagged values, the model has learned how previous energy output affects future values, which is especially useful in energy forecasting, where time-dependent patterns are common. For instance, the lag features up to 12 hours can be expressed as:

$$\mathrm{Lag}_1 = kPt_{t-1}, \quad \mathrm{Lag}_2 = kPt_{t-2}, \quad \ldots, \quad \mathrm{Lag}_{12} = kPt_{t-12} \tag{5}$$

3.3.3. Cyclical encoding of temporal features

Temporal features like the hour of the day, day of the week, and month inherently follow cyclical patterns that repeat over a fixed period. For example, the hour of the day is a cycle that repeats every 24 h. This periodic nature can be effectively modeled using trigonometric functions, specifically sine and cosine, which are inherently periodic.

Consider the hour of the day, which ranges from 0 to 23. To encode this feature, we can use the sine and cosine functions to map the hour onto a unit circle. For example, at 0 hours (midnight), the sine and cosine values would correspond to the angle 0° or 0 radians on the unit circle, giving $(\sin(0), \cos(0)) = (0, 1)$. At 6 h (6 AM), which is one-quarter through the cycle, the angle on the unit circle would be 90° or $\frac{\pi}{2}$ radians, yielding $(\sin(\frac{\pi}{2}), \cos(\frac{\pi}{2})) = (1, 0)$. Similarly, at 12 hours (noon), corresponding to 180° or π radians, the sine and cosine values would be $(\sin(\pi), \cos(\pi)) = (0, -1)$. Finally, at 18 h (6 PM), the values would correspond to 270° or $\frac{3\pi}{2}$ radians, giving $(\sin(\frac{3\pi}{2}), \cos(\frac{3\pi}{2})) = (-1, 0)$. This method enables the model to understand that 23 hours (11 PM) and 0 hours (midnight) are temporally adjacent, a feature that typical one-hot encoding would overlook. Furthermore, this technique is not restricted to hours; it can be used for any cyclical temporal characteristic, such as days of the week or months of the year, ensuring that time's cyclical nature is kept and efficiently utilized in the modeling process.

For example, the encoding of the hour of the day can be defined as:

$$\text{hour\_sin} = \sin\left(\frac{2\pi \cdot \text{hour}}{24}\right) \tag{6}$$

$$\text{hour\_cos} = \cos\left(\frac{2\pi \cdot \text{hour}}{24}\right) \tag{7}$$

Similarly, for the day of the week and month:

$$\text{day\_of\_week\_sin} = \sin\left(\frac{2\pi \cdot \text{day\_of\_week}}{7}\right) \tag{8}$$

$$\text{day\_of\_week\_cos} = \cos\left(\frac{2\pi \cdot \text{day\_of\_week}}{7}\right) \tag{9}$$

$$\text{month\_sin} = \sin\left(\frac{2\pi \cdot \text{month}}{12}\right) \tag{10}$$

$$\text{month\_cos} = \cos\left(\frac{2\pi \cdot \text{month}}{12}\right) \tag{11}$$

For example, if it is 3 PM (15th hour), then:

$$\text{hour\_sin} = \sin\left(\frac{2\pi \cdot 15}{24}\right) \approx 0.866 \tag{12}$$

$$\text{hour\_cos} = \cos\left(\frac{2\pi \cdot 15}{24}\right) \approx -0.500 \tag{13}$$

4. Evaluating demand response for SG for a specific locality

Understanding a grid's demand response is critical for balancing energy supply and demand, maintaining stability, and maximizing resource allocation. While the information in question is restricted to a month's worth of data, it offers a unique chance to examine the grid's performance, particularly regarding energy storage and generation. The existence of a variable indicating positive energy generation is very advantageous. It enables daily data sampling to track the incremental energy stored in the batteries, which can then be used to calculate the average energy delivered to the grid. This conclusion is crucial since it aids in understanding not just consumption patterns but also the efficiency and adequacy of energy generation about grid demand.

Given that the hyperlocal environment is a Taiwanese educational facility, the energy consumption patterns should be unique to its operating dynamics. In previous studies, such as in Wang (2019), authors have measured the demand, providing a basic understanding of the institute's energy use in Mega Watt-hours (MWh). This historical data helps create a baseline against which to evaluate the present dataset's findings.

The temporal changes in energy use and the possibility for scalability need to be examined to understand the grid's demand response better. Energy consumption trends at educational institutions are mainly predictable based on their academic calendar, with fluctuations over weekdays, weekends, and holidays. It may derive not just the average daily supply but also the peak demand periods and the grid's reaction to these changes by examining the daily rise in battery storage (Almazrouee et al., 2020). Furthermore, the scalability of the grid's energy supply is crucial. The grid must adjust as the institute grows or changes its energy usage habits. The data gives a snapshot that may be used to advise future grid expansions or changes to meet shifting demand.

Equation (14) for determining power demand in MWh is based on a well-established formula for energy consumption (Wang, 2019), which considers the facility's overall area and the energy spent per unit area. This equation enables an evaluation of overall energy consumption within the provided time frame.

$$\text{Total Energy Consumption (MWh)} = \left(\frac{\text{Energy Consumption per Unit Area}}{\left(\frac{\text{kWh}}{\text{m}^2\cdot\text{month}}\right)} \right) \times \text{Total Area } (\text{m}^2) \times \frac{1}{1000} \tag{14}$$

5. Experimental evaluation

This study suggests a unique strategy for optimizing power generation in SGs. The strategy uses sophisticated ML algorithms to utilize the synergy between demand response systems and hyperlocal weather forecasts. The primary idea, as proposed in (Shaikh & Khattak, 2024), is to incorporate comprehensive meteorological data into the SG's operational framework, improving the predictability and efficiency of power generation and distribution. ML models are developed and trained using two datasets: time series data for SG battery storage and hyperlocal weather data from a specific locality where the SG is sourced. The complex data integration and model training procedure is carried out to estimate power consumption precisely and optimize energy distribution in SGs.

The research thoroughly examines different ML and time series forecasting models, each chosen for distinct features and applicability for the demanding job. SARIMAX, Prophet, XGBoost, LSTM, and Holt–Winters are among the prospective models, as is a unique hybrid model built to integrate the capabilities of separate models. The flowchart for the overall architecture is given in Figure 4. The comparison of the implementation of all models is shown in Table 3.

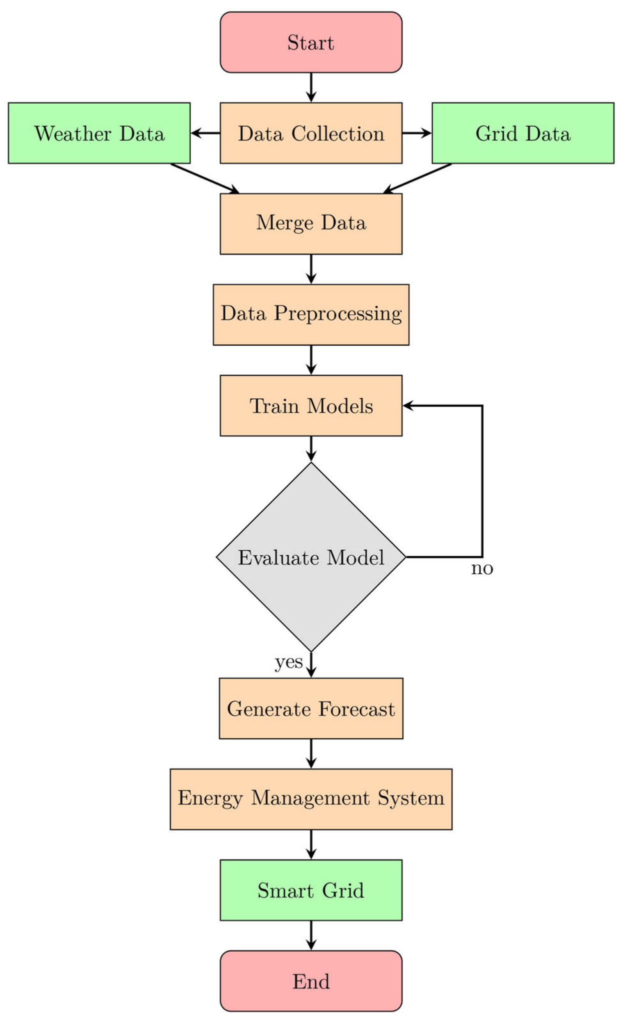

Figure 4. Compact architecture for weather and grid data integration.

Table 3. Implementation and potential comparison of different prediction models.

Model	Configuration	Data preprocessing	Computational complexity	Model potential
SARIMAX	Seasonality, trend, and external variable settings	Time series decomposition, normalization	Moderate, depends on data size and seasonality length	Excels in scenarios with clear seasonal patterns and external influences
Prophet	Flexible seasonality, holiday effects	Minimal, robust to missing data	Low to moderate, scalable	Best for datasets where trend and seasonality are strong predictors
XGBoost	Parameter tuning for depth, learning rate, estimators	Feature engineering, normalization	High, especially with large datasets	Outperforms in predictive power and speed when dealing with large feature sets
LSTM	Network architecture (number of layers, neurons)	Sequence normalization, windowing	High, depends on network complexity	Ideal for sequence prediction problems with long-term dependencies
Holt–Winters	Seasonal and trend components configuration	Seasonal adjustment, normalization	Low, efficient for smaller datasets	Superior in short-term forecasting with regular seasonal cycles
Hybrid Model	Combination of SARIMAX, Prophet, and Holt–Winters settings	As per individual models	Varies, can be high due to multiple models	Optimizes accuracy in complex scenarios by combining multiple model strengths

Table 4. Parameters for SARIMAX model.

Param type	AR order	Integ order	MA order	Seas period
Order	4	1	0	–
Seasonal order	4	1	1	24

The models are trained differently for each approach. The details for each model are given below. Different time series and conventional ML models are deployed to predict and forecast Energy consumption patterns involving weather data. *Absolute power (kPt)* has been chosen as the dependent variable.

5.1. Seasonal autoregressive integrated moving average (SARIMAX) model

SARIMAX has been used as the data shows seasonality, and using just ARIMA did not justify results as simple ARIMA does not support most of the time series components that this data possesses. As the SG battery data has been integrated with exogenous factors, i.e., weather variables, the best time series approach can be SARIMAX (Elshewey et al., 2022). Cyclic encoding for an hour, day of week, and month has been used in addition to exogenous factors to improve the previous methodologies and to have the best possible results.

Except for the past 24 hours, saving for the testing set, the training set contains all data points. Specific parameters are set in the model to accommodate autoregressive terms, differencing, moving average terms, and seasonality. The model improves forecasting performance by handling autoregressive (AR), moving average (MA), and seasonal components. The model iteratively modifies these parameters using maximum likelihood estimation, reducing the difference between projected and actual values. Furthermore, it adds exogenous meteorological variables into its regression framework, allowing the model to understand how weather changes affect energy usage. A grid search technique has also been integrated to tune hyperparameters such as AR terms (p), MA terms (q), and seasonality (P) to improve the model's predicting power. Also, the cyclic encoding, as explained in Section 3.3.3, was employed and proved to reduce the error metrics for the model.

Equation (15) shows the notation of the SARIMAX model used in the model. Table 4 shows the parameters used in the model training.

$$\begin{aligned}\Delta^d \Delta_s^D y_t = \alpha + \sum_{i=1}^{p} \phi_i y_{t-i} + \sum_{j=1}^{q} \theta_j \varepsilon_{t-j} \\ + \sum_{i=1}^{P} \Phi_i y_{t-i\times s} + \sum_{j=1}^{Q} \Theta_j \varepsilon_{t-j\times s} + \beta X_t + \varepsilon_t\end{aligned} \tag{15}$$

where:

- y_t is the observed time series data at time t,
- ϕ_i are autoregressive terms,
- θ_j are moving average terms,
- s is the seasonal period,
- X_t are exogenous variables (i.e., weather data).

5.2. Facebook Prophet model

Facebook's Prophet model is a powerful forecasting tool for time series data with significant seasonal trends and numerous seasons. It is especially well-suited for data with daily observations containing missing values and unique occurrences that may impact trends (Kumari et al., 2022). The time series decomposition model integrates trend, seasonality, and holiday impacts, providing flexibility and simplicity of understanding. The Prophet model was chosen for this approach next to SARIMAX because of its ability to manage the dataset's complicated seasonal cycles.

The dataset is reconstructed to meet the Prophet model's input requirements. The data frame has the date, target variable, and exogenous attributes labeled suitably to help the model identify and handle the data items. The model is configured to account for daily and weekly seasonality, ensuring that the model captures intrinsic patterns and swings at multiple time scales. Exogenous variables are added as regressors to improve the model's prediction accuracy by accounting for external factors.

In addition to the usual seasonality, weekly cycles and finer-grained daily seasonalities utilizing the Prophet's custom seasonalities were introduced, as shown:

```
m.add_seasonality(name='weekly', period = 7, fourier_order = 3)
m.add_seasonality(name='daily', period=1, fourier_order=10)
```

This helps capture the influence of repeating weekly patterns, such as differences in energy usage between weekdays and weekends and daily patterns representing hourly consumption fluctuations.

The implementation of Prophet combined with hyperlocal weather data is shown in Eqs. (16)–(20).

$$y(t) = g(t) + s(t) + h(t) + \varepsilon_t \tag{16}$$

Equation (17) shows the trend component, Eq. (18) shows the seasonality component and Eq. (19) shows the holiday trend used in the model to catch the trend and seasonality from the time series data. Equation (20) shows the method by which exogenous variables are included in the model training.

$$g(t) = \frac{C}{1 + e^{-k(t-m)}} \tag{17}$$

where:

- C: Carrying Capacity
- k: Growth Rate
- m: Offset Parameter

$$s(t) = \sum_{n=1}^{N} \left(a_n \cos\left(\frac{2\pi nt}{P}\right) + b_n \sin\left(\frac{2\pi nt}{P}\right)\right) \tag{18}$$

where:

- P: Period (e.g., 30 for monthly seasonality)
- a_n and b_n: Fourier coefficients

$$h(t) = \sum_{i=1}^{H} I(t \in \text{Holiday}_i) \cdot \delta_i \tag{19}$$

The holiday effect $h(t)$ is modeled as an indicator function that adds a constant effect for holidays.

where:

- I: Indicator function
- Holiday$_i$: Represents each holiday
- δ_i: Effect of the th holiday

$$y(t) = g(t) + s(t) + h(t) + \beta X(t) + \varepsilon_t \tag{20}$$

where:

- $X(t)$: Represents the Exogenous variables
- β: Vector of coefficients for these variables

5.3. Holt–Winters exponential smoothing model

Particularly for data with seasonality and trend, the Holt–Winters exponential smoothing model goes beyond conventional exponential smoothing by including trend and seasonality components, making it a powerful tool for forecasting complicated time series data. The Holt–Winters model is chosen for its ability to capture and model the dataset's complex patterns of seasonality and trend. The model's ability to generate accurate short-term forecasts and ease of implementation make it a popular choice for energy consumption and generation forecasting. The parameters for the model are shown in Table 5. The model's additive nature shows a linear trend and seasonality, making it suited for datasets with these components changing consistently (Almazrouee et al., 2020). The 24 seasonal periods demonstrate the model's flexibility to datasets with diverse seasonal patterns, reflecting the hourly data's underlying daily changes.

Equation (21) shows the level; Eq. (22) shows the trend, Eqs. (23) and (24) show the daily and weekly seasonal components used, and Eq. (25) shows the forecast equation. Whereas Table 5 shows the parameters used in the model.

$$l_t = \alpha(y_t - s_{t-P}) + (1-\alpha)(l_{t-1} + b_{t-1}) \tag{21}$$

where:

- α: Smoothing parameter for the level between 0 and 1.
- y_t: Observed values at time t.
- s_{t-P}: Seasonal component at time $t-P$, where P is the seasonal period.

$$b_t = \beta^*(l_t - l_{t-1}) + (1-\beta^*)b_{t-1} \tag{22}$$

where:

- β^*: Smoothing parameter for the trend, between 0 and 1.

$$s_{t,\text{daily}} = \gamma(y_t - l_t) + (1-\gamma)s_{t-24} \tag{23}$$

$$s_{t,\text{weekly}} = \gamma_w(y_t - l_t) + (1-\gamma_w)s_{t-168} \tag{24}$$

where:

- γ: Smoothing parameter for daily seasonality.

Table 5. Parameters for Holt–Winters model.

Parameter	Value
Trend	Additive
Seasonality	Additive
Seasonal periods	24

- γ_w: Smoothing parameter for weekly seasonality.

$$\hat{y}_{t+h|t} = l_t + hb_t + s_{t+h-P} \tag{25}$$

where:

- h: Forecast horizon (the number of steps ahead).
- s_{t+h-P}: Seasonal component adjusted for future time steps.

The last three models used are purely time series models. All three of these models have performed up to the mark, but out of curiosity and better comparison, playing with conventional ML models will make no loss.

5.4. XGBoost model

XGBoost (Extreme Gradient Boosting) is a well-known ML method that is particularly well-liked for its performance and quick training. It is a fast and efficient implementation of gradient-boosted decision trees. Because of its capacity to handle multiple forms of structured data well, XGBoost can be especially useful in time series forecasting. It can take missing values and help with tree-building parallelization (Łoś et al., 2021).

The XGBoost model predicts power generation by first dividing it into training and testing sets. Based on the MAE criteria, the model is subjected to hyperparameter tuning using GridSearchCV to determine the ideal parameters that produce the most outstanding performance. The ideal parameters are then utilized on the training data to train the XGBoost model. Exogenous features such as temperature, humidity, wind speed, cloud cover, and cyclical encoding of time variables such as hour, day of the week, and month are used to train the model. The trained model is then used to forecast data for the following 24 hours. In addition to the basic XGBoost, the model was improved using lag features from Section 3.3.2 (prior power usage data) and engineered features from the meteorological dataset (temperature, humidity, and wind speed).

New weather-related elements were included to simulate the impact of meteorological conditions on energy use which includes:

- Temperature Difference: Difference between maximum and minimum temperature during the day.
- Humidity Range: Range of humidity values during the day.

XGBoost optimizes a composite objective function consisting of a loss function and a regularization term. The objective function at iteration t is represented in Eq. (26). While the Table 6 gives the parameters used in the implementation.

$$\begin{aligned} \mathrm{Obj}^{(t)} &= \sum_{i=1}^{n}\left(y_i - \left(\widehat{y_i^{(t1)}} + f_t(x_i)\right)\right)^2 \\ &+\lambda\sum_{j=1}^{T} w_j^2 + \alpha\sum_{j=1}^{T}|w_j| \end{aligned} \tag{26}$$

Where:

- y_i: Actual Value
- $\widehat{y_i^{(t1)}}$: Predicted Values at Iteration $t-1$
- $f_t(x_i)$: Decision Tree Output at iteration t

Table 6. Parameters for Holt–Winters exponential smoothing model.

Parameter	Value
Max depth	3, 5, 7
Number of estimators	50, 100, 200
Learning rate	0.01, 0.1, 0.2
Cross-validation	3-fold
Scoring metric	Negative mean absolute error

- λ, α: Regularization Parameters
- w_j: Weight of jth leaf in the tree
- T: Number of leaves in the tree

Further, the XGBoost in this approach uses first- and second-order derivatives (Gradient and Hessian) for optimization. For a given loss function l, the gradient and Hessian are given in Eqs. (27) and (28).

$$g_i = \partial_{\widehat{y^{(t1)}}} l(y_i, \widehat{y_i^{(t1)}}) \tag{27}$$

$$h_i = \partial^2_{\widehat{y^{(t1)}}} l(y_i, \widehat{y_i^{(t1)}}) \tag{28}$$

whereas the score of Tree Structure Q in this model is given in Eq. (29).

$$\text{Score}(Q) = -\frac{1}{2}\sum_{j=1}^{T} \frac{G_j^2}{H_j + \lambda} \tag{29}$$

where:

- G_j: Sum of Gradients in jth leaf.
- H_j: Sum of Hessians in the jth leaf.
- λ: L2 Regularization parameter.

After dealing with three time series and one conventional ML model, it has been noticed that there might be a need to add a DL model to know if it performs better than the traditional ML model. DL models are used because of their capacity to predict complicated, non-linear connections in data, which is especially useful for time series forecasting. DL models, such as LSTM, can grasp subtle patterns and temporal relationships (Dudek et al., 2022) in terms of forecasting values, and providing improved accuracy. These models extract useful characteristics automatically, reducing the need for human feature engineering, and can handle massive amounts of data, enhancing prediction, precision and dependability.

5.5. Long short-term memory (LSTM) model

The basic concept underlying LSTM is a memory cell that stores necessary information throughout the sequence's processing and non-linear gating units that govern information flow in the cell (Dudek et al., 2022). Long-term temporal associations can be recorded by memory, and the effects of short-term memory can be decreased, i.e., information from earlier time steps can find its way to later time steps. LSTMs are notable for their capacity to capture and represent complex patterns and temporal relationships in sequential data, providing better performance and accuracy in various applications. They are trained to utilize back-propagation across time (Livieris et al., 2021). An LSTM cell has three gates: input, forget, and output, as well as two states, i.e., cell state, and hidden state.

The equation for forget gate is shown in Eq. (30), the input Gate in Eq. (31), the candidate layer in Eq. (32), the cell state update in Eq. (33), and the output gate in Eq. (34). Whereas, the parameters used in the model are shown in Table 7.

In this case, LSTM estimates the batteries' power when exogenous factors, such as weather data, are introduced. The LSTM model may discover patterns in data that are too complicated or have too many sequential relationships for simpler models.

A few enhancements were made to improve the standard LSTM model:

- The LSTM uses historical energy usage data, hyperlocal weather variables (temperature, humidity, wind speed, cloud cover), and cyclically encoded time features (hour of the day and day of the week) from Section 3.3.3.

Table 7. Parameters for long short-term memory (LSTM) model.

Parameter	Value
Input shape	(1, 30)
LSTM units	100
Dense units	4
Loss function	Mean squared error
Dropout rate	0.2
Optimizer	Adam
Learning rate	0.001 (optimized via Bayesian optimization
Batch size	10
Lookback window	30 time steps
Epochs	100

- An attention mechanism was included to allow the model to focus on crucial periods (for example, peak hours) rather than evenly considering all past data points. The attention mechanism computing the context vector is shown in Eq. (35).
- Bayesian optimization was used to fine-tune parameters, including the number of LSTM layers, neurons per layer, dropout rates, and learning rate.
- The LSTM model was configured to predict multiple time steps.

$$f_t = \sigma(W_f \cdot [h_{t-1}, x_t] + b_f) \tag{30}$$

$$i_t = \sigma(W_i \cdot [h_{t-1}, x_t] + b_i) \tag{31}$$

$$\tilde{C}_t = \tanh(W_C \cdot [h_{t-1}, x_t] + b_C) \tag{32}$$

$$C_t = f_t * C_{t-1} + i_t * \tilde{C}_t \tag{33}$$

$$o_t = \sigma(W_o \cdot [h_{t-1}, x_t] + b_o) \tag{34}$$

$$context_t = \sum_{i=1}^{T} \alpha_i h_i \tag{35}$$

5.6. Hybrid time series model with dynamic re-calibration

The hybrid model, which combines the SARIMAX, Holt–Winters, and Prophet models, exemplifies the constructive interaction of many forecasting methodologies, each providing unique characteristics to improve overall predicted accuracy. SARIMAX excels in capturing complicated seasonal patterns and auto-correlations, which may be attributed to its robust parameterization and incorporation of exogenous factors. However, its effectiveness can be limited by non-linear patterns and numerous seasonalities, which can be effectively handled using the Prophet model. Despite its adaptability, Prophet can be computationally demanding and may not always yield the best match, particularly in instances with complex data patterns and anomalies. The Holt–Winters model complements the hybrid ensemble's capacity to capture level, trend, and seasonality. While it excels at detecting systematic patterns in data, its performance might suffer when dealing with several seasonal patterns or non-linear trends.

The novelty is that this approach includes a dynamic recalibration mechanism that modifies each model's weights depending on its most recent prediction performance. This recalibration method increases models' weights with fewer predicting errors while penalizing poorly performing models. The weights are adjusted proportionately to the inverse of each model's error, ensuring the models that contribute the most to correct forecasts are prioritized in subsequent predictions. The recalibration occurs depending on performance across a sliding window of size *N*. This allows the model to alter its weights in response to current performance patterns, guaranteeing that it can react to short-term data fluctuations. This technique eliminates over-reliance on any particular model in the long run and assures response to shifting data trends.

In addition to dynamic recalibration, the hybrid model uses a self-learning algorithm to fine-tune model parameters depending on error feedback. As new data becomes available, the hybrid model dynamically modifies its parameters, improving real-time forecast accuracy. The hyperparameters used in the models are as follows:

- Learning rate δ: Determines how aggressively the model adjusts weights in response to performance changes.
- Window size N: Defines the number of recent predictions considered during recalibration.
- Initial weights w_1, w_2, w_3: The starting weights for SARIMAX, Holt–Winters, and Prophet, respectively. These weights are dynamically adjusted as the model learns from performance data.

The recalibration technique is shown as:

$$w_i(t+1) = w_i(t) \cdot \left(1 + \delta \cdot \frac{e_{\min}}{e_i(t)}\right) \tag{36}$$

where:

- $w_i(t+1)$ is the recalibrated weight for model i at the next time step,
- $w_i(t)$ is the current weight of model i,
- δ is a learning rate or scaling factor controlling the magnitude of recalibration,
- $e_{\min}$ is the minimum error across all models in the current time window,
- $e_i(t)$ is the error for model i at time t.

This approach ensures the hybrid model is adaptive and robust. It can recalibrate itself to optimize forecasting performance in real-time, making it well-suited for the highly dynamic environment of power generation forecasting.

The parameters for the model are shown in Table 8.

6. Results and evaluation

The dataset was split into training, validation, and test sets to evaluate the models and ensure robust performance. Specifically, we used a 70-15-15 split, where 70% of the data was used for training, 15% for validation, and the remaining 15% for testing. This approach allows us to train the model, tune hyperparameters, and assess the final performance on unseen data. The validation set was used to fine-tune the model parameters and prevent overfitting, while the test set provided an unbiased evaluation of the model's accuracy.

The performance evaluation metrics are crucial for evaluating the ML models helping us better understand where a specific model is outperforming and where it is lacking, compared to other models. The following metrics are used to evaluate the models.

1. **Mean Absolute Error (MAE)** measures the average magnitude of the errors in a set of predictions without considering their direction. It is calculated as:

$$\text{MAE} = \frac{1}{n}\sum_{i=1}^{n}|y_i - \hat{y}_i| \tag{37}$$

Table 8. Hybrid model parameters.

Model	Parameter	Description	Value
Prophet	Daily seasonality	Whether to include daily seasonality	True
SARIMAX	Order	The order of autoregression, integration, and moving average components	(4,1,0)
	Seasonal order	Order of seasonal components	(1,4,24)
	Disp	Whether to display convergence statistics	False
Holt–Winters	Trend		Additive
	Seasonal		Additive
	Seasonal periods	Number of periods in a complete seasonal cycle	Depending on the number of hours of forecast desired, i.e., 1,2,3,12,24,36

2. **Mean Squared Error (MSE)** is the average of the squares of the errors, giving more weight to larger errors, and is calculated as:

$$\mathrm{MSE} = \frac{1}{n}\sum_{i=1}^{n}\left(y_i - \widehat{y}_i\right)^2 \tag{38}$$

3. **Root Mean Squared Error (RMSE)** is the square root of the MSE and gives an error metric in the same units as the target variable. It is calculated as follows:

$$\mathrm{RMSE} = \sqrt{\frac{1}{n}\sum_{i=1}^{n}\left(y_i - \widehat{y}_i\right)^2} \tag{39}$$

4. **Mean Absolute Percentage Error (MAPE)** measures the average percentage error and is calculated as:

$$\mathrm{MAPE} = \frac{100\%}{n}\sum_{i=1}^{n}\left|\frac{y_i - \widehat{y}_i}{y_i}\right| \tag{40}$$

5. ***R*-squared Score** indicates how well the model's predictions fit the actual data. It is calculated as:

$$R^2 = 1 - \frac{\sum_{i=1}^{n}\left(y_i - \widehat{y}_i\right)^2}{\sum_{i=1}^{n}\left(y_i - \overline{y}\right)^2} \tag{41}$$

6.1. Evaluation of SARIMAX model

The SARIMAX model forecasts the next 24 hours of data following successful training. The projection considers the testing set's exogenous properties to achieve accuracy. The two Figures 5 and 6 show how a SARIMAX model predicts kilowatt-hour (kPt) production for an SG system.

The absolute kPt values are presented with the SARIMAX predicted values across multiple days in Figure 5. The actual data displays substantial changes, with peaks and troughs indicating fluctuating power production due to demand cycles or variations in renewable energy supply. The SARIMAX forecast, shown by a dashed line with cross symbols, matches these actual values closely, with a shaded forecast region reflecting the confidence interval around the estimates. The overlap between anticipated and actual values indicates the model successfully captured time series dynamics up to the end of the observed data.

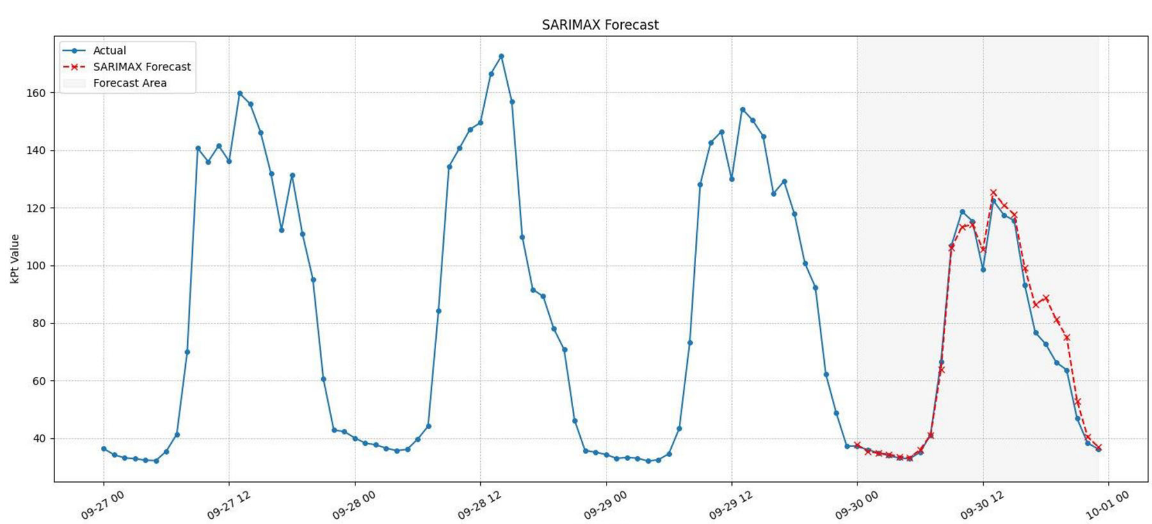

Figure 5. SARIMAX model forecast (24 hours).

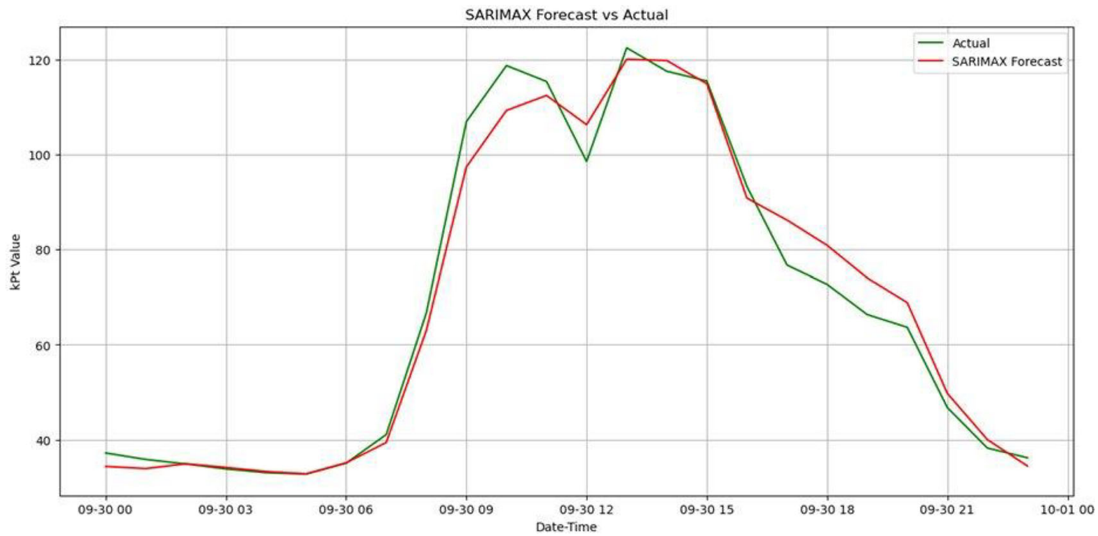

Figure 6. SARIMAX fit on data (24 hours).

Table 9. Performance evaluation metrics for machine learning models based on a 24-hour forecast horizon (higher is better for *R*-squared score, and lower is better for MAE, MSE, RMSE, and MAPE).

Model	MAE	MSE	RMSE	MAPE (%)	*R*-squared
SARIMAX	3.54	22.97	4.79	4.92	0.97
FBProphet	6.17	62.9	7.93	9.22	0.88
Holt–Winters	5.12	67.49	8.21	5.45	0.93
XGBoost	8.24	181.17	13.46	9.78	0.74
LSTM	5.06	62.92	7.93	6.91	0.96
Hybrid model	4.74	47.33	6.88	6.00	0.96

Figure 6 focuses on a shorter period and compares actual and anticipated kPt values more thoroughly. The projection closely resembles the data trend, accurately tracking the rise and decrease in power generation.

The error metrics presented quantitatively evaluate the model's prediction performance in Table 9. The error metrics show predictive solid performance: an MAE of 3.54 indicates that the model's forecasts are only 3.54 kilowatt-hours off from the actual figures on average, indicating a high level of forecast precision. Although the MSE is moderate at 22.97, it means the presence of specific predictions with significant errors due to the squaring of error factors. This is supported by an RMSE of 4.79, indicating that the model's forecasts may occasionally deviate from actual values. Nonetheless, a MAPE of 4.92% suggests a relatively good model, with projections often departing from actual values by less than 5%.

6.2. Evaluation of FB Prophet model

The forecast plots showing (trend, forecast for the day of week, forecast for the day of year, forecast for the hour of the day, and extra additive regressors) for power generation are shown in Figure 7. In contrast, Figure 8 shows the forecast showing actual and predicted patterns over the data.

The two charts (7 and 8) and error metrics (Table 9) are related to the use of the Prophet forecasting model in estimating kilowatt-hour (kPt) generation for an SG system, keeping in view the meteorological data. Figure 7 shows the actual and anticipated kPt values over a month, with the Prophet forecast closely mirroring the observed values. Though there are instances of substantial variation, the prediction line reflects the rhythm and peaks of power output.

Figure 8 breaks down the prediction into its constituent parts: trend, weekly seasonality, yearly seasonality, daily patterns, and various regressors that may account for holidays or other unique occurrences. The trend component exhibits a declining pattern during the month, which indicates a seasonal decrease in power generation or an underlying negative tendency in the data. Weekly seasonality

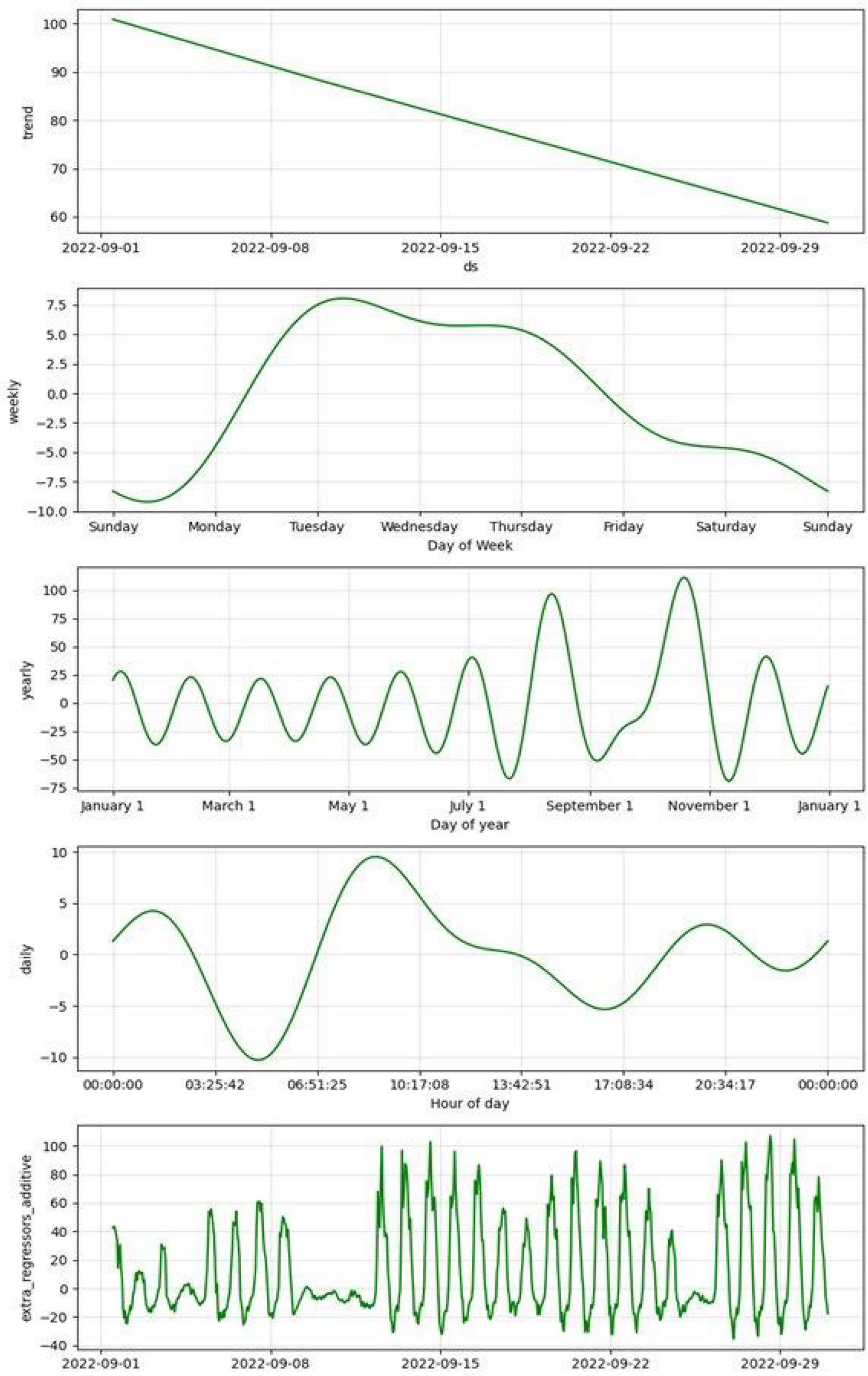

Figure 7. Forecast plots for prophet model.

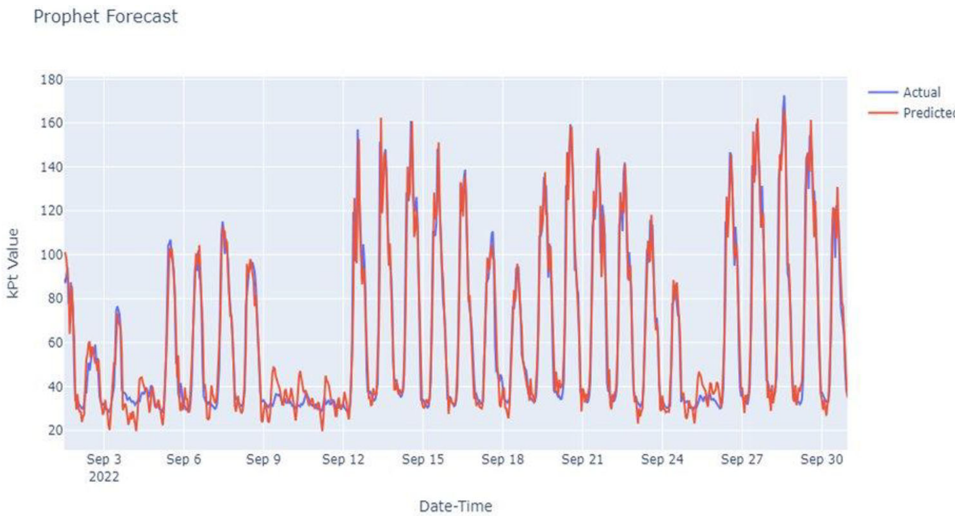

Figure 8. Prophet forecast (24 hours).

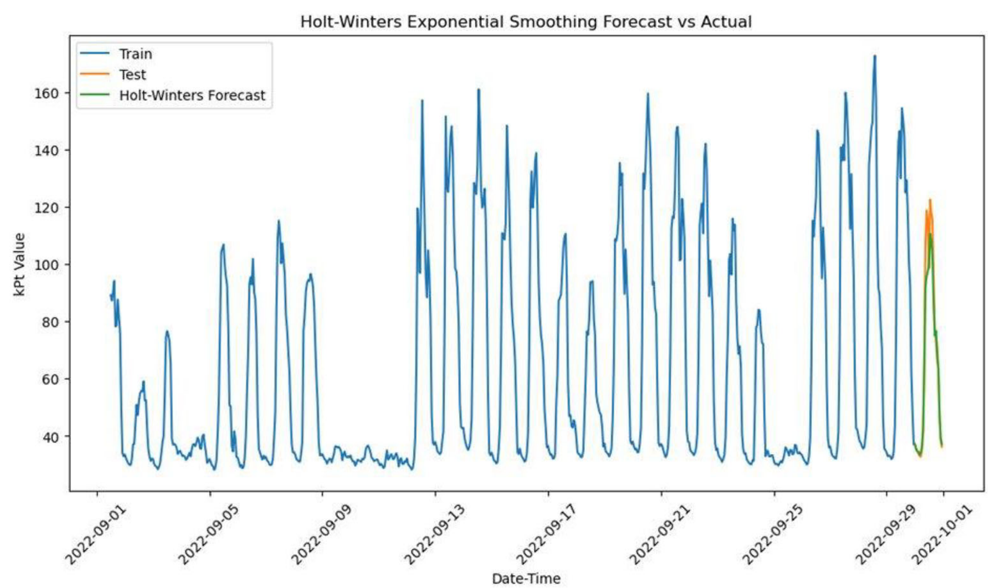

Figure 9. Holt–Winters exponential smoothing forecast (24 hours).

follows a consistent pattern, suggesting regular variations within days of the week. Yearly and daily components reveal the effect of longer-term cycles and within-day patterns on electricity generation.

An MAE of 6.17 indicates that the forecast deviates from the actual values by this amount on average, which, given the kPt value scale, may reflect a considerable level of error. The MSE of 62.9, a higher number owing to error squaring, indicates that more significant errors have a greater influence on the model's performance. Substantial forecast errors are confirmed by an RMSE of 7.93, more than the MAE. The MAPE of 9.22% indicates that the model's predictions are often within 9.22% of the actual values showing the model is moderately accurate in relative terms but might benefit from more accuracy for more precise energy management methods.

6.3. Evaluation of Holt–Winters exponential smoothing model

The performance of a Holt–Winters exponential smoothing model is depicted in Figures 9 and 10, and the accompanying error metrics are included in Table 9. Because it extends exponential smoothing to capture seasonality in addition to trends, the Holt–Winters approach is particularly well-suited to time series data having a seasonal pattern.

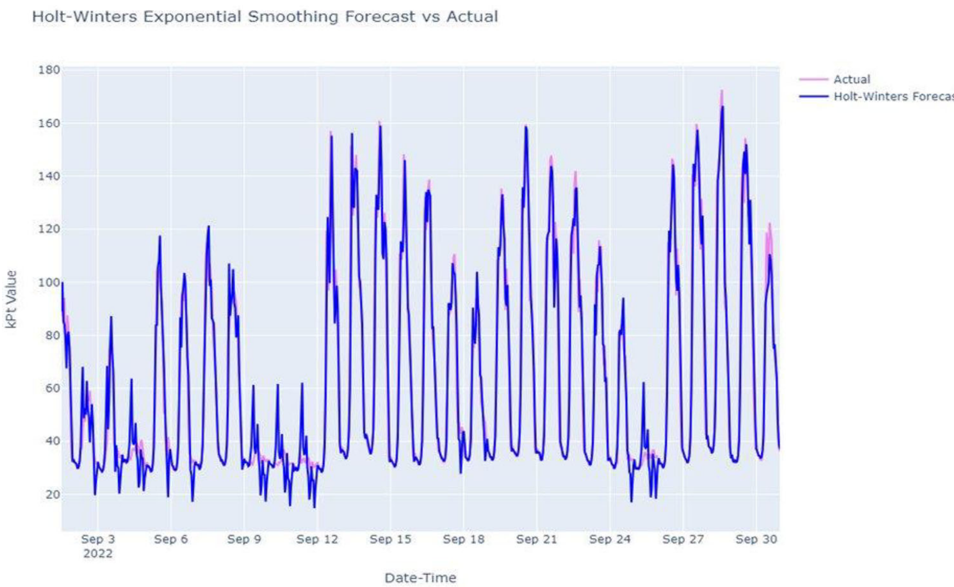

Figure 10. Holt–Winters exponential smoothing model's fit on data.

The actual power-generating data, shown as a solid blue line in Figure 9, demonstrates a distinct periodic pattern, typical of power use cycles primarily impacted by consumer behavior, industrial demand, or the availability of RESs. The orange line represents the model's forecast, which closely corresponds with the actual data during the training phase and extends into the test phase with green, indicating the model's ability to predict future values based on learned previous patterns. Figure 10 emphasizes the model's predicting abilities, with projected values nearly mirroring the actual data, with occasional variations indicated. The projected values represent the model's effort to match the accurate kPt generation data's cyclical peaks and troughs.

An MAE of 5.16, which differs from the actual values by an average of 5.16 kPt, indicates moderate accuracy in SG power generation. The MSE of 68.11 suggests the presence of some significant errors due to the model's susceptibility to abrupt changes in power generation that the seasonal and trend components of the model do not capture. An RMSE of 8.25 indicates the presence of more considerable errors while still indicating that the model is typically dependable in its predictions. Last, the MAPE of 5.58% suggests that the model's estimates are usually within 5.58% of the actual data, which is sufficient for many practical applications in SG management.

6.4. Evaluation of XGBoost model

The XGBoost model, as shown in Figures 11 and 12, has been used to anticipate power generation in an SG system, keeping the weather patterns in view. The projection in Figure 11 goes beyond the previous data utilized for training and testing. While the anticipated numbers may not fully match the actual data, they show some unity, particularly in reflecting power generation's overall pattern and periodicity. Figure 12 further emphasizes the model's efficiency, comparing the model's full-month forecast to actual data. Despite minor variances, the anticipated pattern matches the actual data, indicating that the model has sufficiently internalized the cyclic behavior of the power-generating process. Error measures examine the model's predicted accuracy quantitatively, as shown in Table 9.

The model's average deviation from the actual data is moderate, as indicated by an MAE of 8.24, which may be acceptable within specified operating conditions. Further, MSE and RMSE of 181.17 and 13.46 suggest the presence of significant individual forecasting errors, emphasizing potential outlier occurrences or model sensitivity concerns. Whereas an MAPE of 9.78% represents a moderate relative error margin, suggesting that while the model is usually effective at monitoring the data trend, accuracy might be improved in some areas.

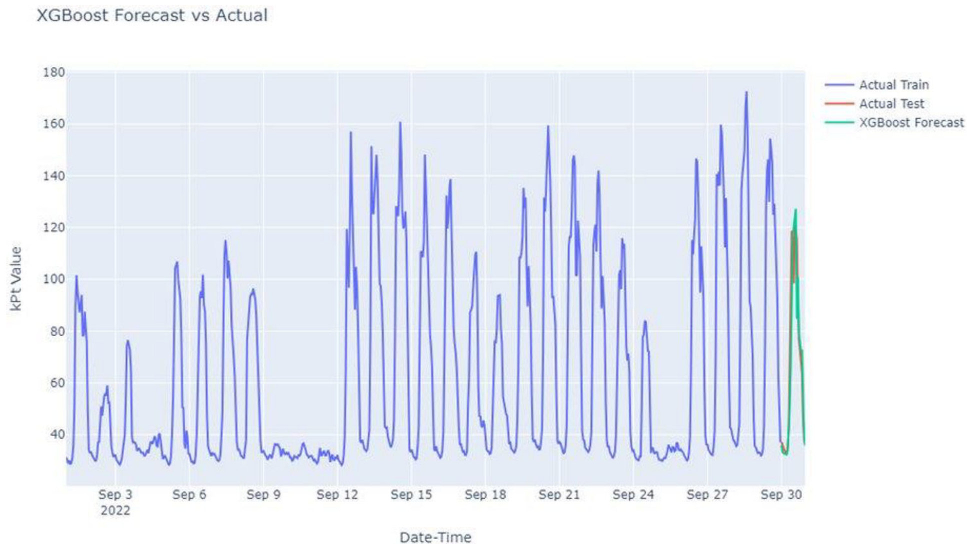

Figure 11. XGBoost model forecast (24 hours).

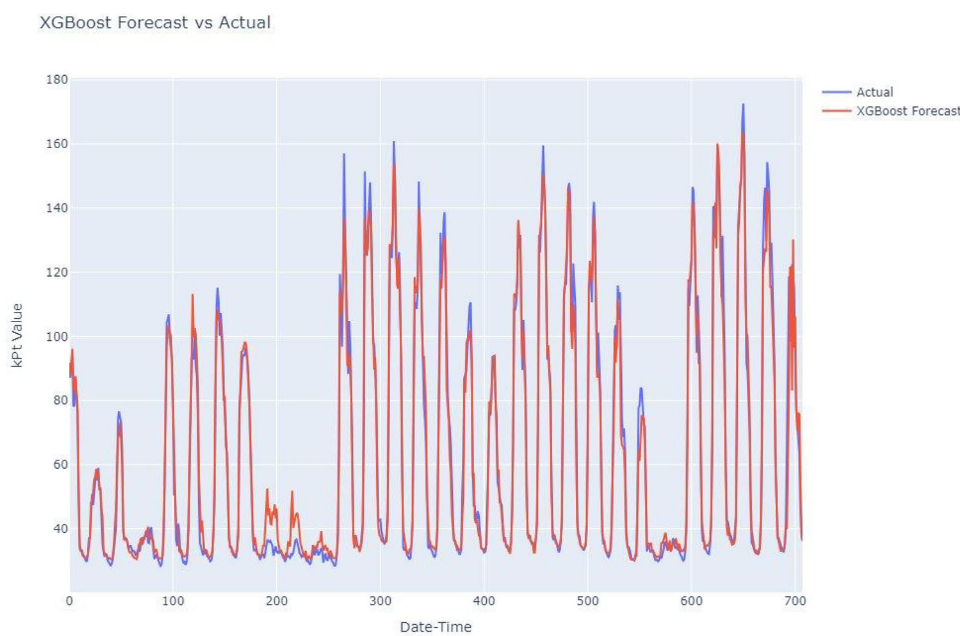

Figure 12. XGBoost forecast vs. actual data.

6.5. Evaluation of long short-term memory (LSTM) model

The LSTM model predicts the kPt values shown in blue alongside the actual kPt values shown in purple as shown in Figure 13. The model's forecasts closely track actual kPt data, precisely capturing peaks and troughs. However, certain anomalies occur when the forecast either underestimates or overestimates the exact numbers, which is especially visible during rapid fluctuations in power generation. The following error measures are used to quantify forecast performance included in Table 9.

An MAE of 5.06 suggests that the model's predictions differ from the actual values by an average of 5.06 kPt, indicating a relatively tight forecast that roughly matches the exact results. The MSE of 62.92, highlights the cumulative impact of forecast errors, emphasizing the presence of specific projections that deviate significantly from actual values. The RMSE is 7.93; indicating the model is typically trustworthy, there are times when its predictions considerably diverge from the actual data. According to the MAPE, the model's projections are within 6.91% of the exact values, indicating an acceptable degree of accuracy in terms of SG forecasting.

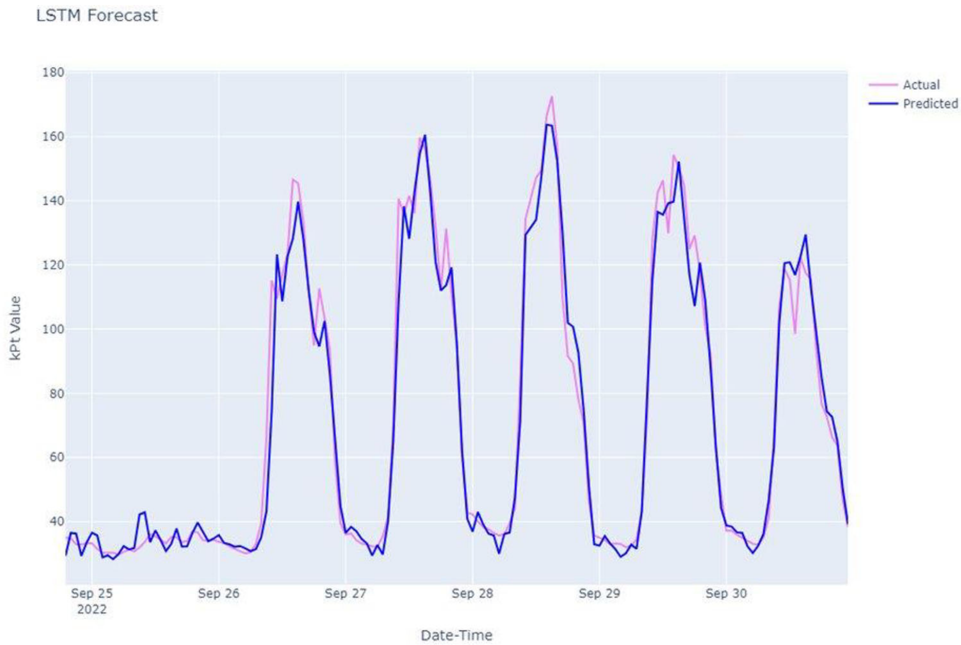

Figure 13. LSTM forecast vs. actual data.

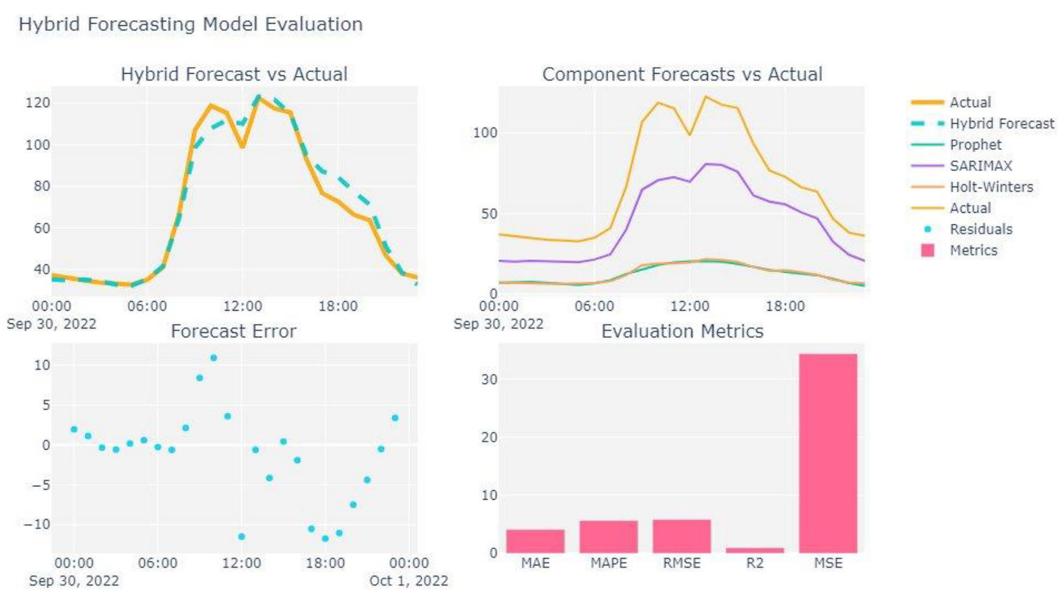

Figure 14. Hybrid model forecast for the next 24 hours.

These insights from the LSTM model's performance are critical for operational decision-making in an SG scenario. The model's capacity to estimate power generation with moderate accuracy may be instrumental in controlling supply and demand, scheduling maintenance, and optimizing resource allocation. The LSTM model's low error rates imply that it might be a reliable tool for predictive analysis in SG operations, with additional tweaking possibly improving accuracy and dependability.

Table 9 shows the Evaluation of all models in terms of metrics, i.e., MAE, MSE, RMSE, MAPE, and R^2 score.

6.6. Evaluation of the hybrid model

While the model can take any number of hours as input, a maximum of 48 hours is recommended. The hybrid model is trained based on the specified input hours, with the data tailored for that specific

Table 10. Training time comparison for models.

Model	Training time (min)
SARIMAX	6
LSTM	5
Holt–Winters	2
XGBoost	8
FBProphet	1.5
Hybrid model	3–4

duration. However, it is essential to note that the primary focus of this research is STLF, which typically yields the most accurate results for a shorter duration. Figure 14 shows the model's output for 24 hours.

The modular design of real-time dashboard guarantees that it can be adjusted to the individual needs of various operators, providing flexibility in the presentation of key performance indicators (KPIs) and allowing operators to alter forecasting parameters without requiring extensive technical expertise. To accommodate operators with no background in ML or meteorology, the dashboard includes straightforward visualization capabilities that instantly translate complicated forecasting data into actionable insights, allowing operators to make real-time decisions without having to interpret raw data. The integration of multiple forecasting models i.e., a hybrid method, improves the system's versatility by allowing different operators to prioritize different models based on grid features.

The top-left subplot compares the hybrid model's predicted values (dashed lines) to the observed values (solid lines). This visual representation aids in immediately determining how closely the model matches the actual data. Deviations between the two lines reflect when the model struggled to match the actual data, which can help identify areas for model development.

The top-right subplot compares individual component forecasts (SARIMAX, Prophet, and Holt–Winters) to the actual data. Visualizing these several model outputs together makes it easier to determine which model component contributed the most to the hybrid forecast's accuracy. For example, if one model continually over- or under-predicts, it may indicate that the hybrid approach's specific component needs to be recalibrated.

The residuals, or disparities between actual and predicted values, are displayed in the bottom-left subplot. This offers information on the error distribution and trends. A well-performing model should have residuals centered around zero with a little volatility. Any notable trends or patterns in residuals may suggest under-fitting or overfitting. By integrating this sub-plot, the dashboard makes anomaly identification and model adjustment easier, which can be critical for real-time decision-making in energy management, offering non-experts and technical operators the tools they need to properly manage grid operations, with a focus on accessibility and adaptability.

The sub-plot on the bottom right shows the error evaluation and scoring metrics. Each of these evaluation criteria offers a unique viewpoint on model accuracy, and when combined, they provide a complete picture of how well the hybrid model works.

6.7. Model training time comparison

When evaluating model accuracy and predicting performance, it is also vital to consider each model's computing efficiency. The time it takes to train each model is critical in real-time energy forecasting, particularly when frequent retraining is required due to new incoming data. Table 10 shows the time required for each model to train using the same train–test–validation split (70-15-15).

The variations in training time-frames between models can be related to their underlying complexity, feature engineering, and computational requirements. SARIMAX, which took 6 minutes, integrates autoregressive, moving average, and exogenous weather factors, making it computationally expensive because it predicts seasonality and trends using precise exogenous data. LSTM took 5 min due to its DL architecture tailored for sequential data, which handles long-term dependencies while being computationally efficient with contemporary python libraries. XGBoost is the most computationally demanding, taking 8 min, because of the vast number of decision trees it trains, particularly with hyperparameter adjustment for depth, learning rate, and estimators. Meanwhile, FBProphet is meant to manage trend and seasonality rapidly with pre-tuned defaults and little feature engineering, which takes only one to two minutes. Holt–Winters, which also integrates trend and seasonality, takes 2 min due to its more straightforward model structure. The Hybrid model, which took 3–4 min, balances complexity by using the benefits of SARIMAX, Holt–Winters, and FBProphet, recalibrating weights dynamically to enhance prediction accuracy while minimizing training time.

6.8. Time and space complexity evaluation

Time complexity defines how long an algorithm takes to execute, whereas space complexity describes how much memory it uses. Low-complexity models are time and memory-efficient, making them appropriate for quicker jobs. More complicated models need more time and memory but provide higher accuracy and flexibility, making them appropriate for resource-intensive jobs.

- SARIMAX's time complexity is quadratic at $\mathcal{O}(n^2)$ due to iterative parameter estimation, mainly when exogenous variables are included (Shannon, 2019). The computational complexity includes linear space complexity $\mathcal{O}(n)$ due to the necessity to store matrices and parameter estimations during training.
- Holt–Winters is computationally efficient, with linear time and space complexity of $\mathcal{O}(n)$, due to its more straightforward structure for simulating seasonality and trend.
- LSTM's DL architecture has a time complexity of $\mathcal{O}(T \cdot n \cdot m)$, where T is the number of time steps, n the number of data points, and m the number of features or hidden units. Its space complexity is also $\mathcal{O}(T \cdot n \cdot m)$, which necessitates storing intermediate state information while training.
- XGBoost's time complexity is $\mathcal{O}(k \cdot d \cdot n \cdot \log n)$, where k is the number of trees, d is the tree depth, and the logarithmic factor originates from determining the optimal split during tree creation. Its space complexity is high, $\mathcal{O}(k \cdot d \cdot n)$, because it has to store trees and intermediate calculations.
- FBProphet, built for quick trend and seasonality modeling, is economical with linear time complexity $\mathcal{O}(n)$. It fits additive models with low storage needs, resulting in a linear space complexity of $\mathcal{O}(n)$.
- The Hybrid Model, which integrates different approaches like SARIMAX and Holt–Winters, adds a reasonable cost with recalibration, giving it a time complexity of $\mathcal{O}(m \cdot n)$, where m represents the recalibration overhead. Similar to its components, its space complexity is linear, $\mathcal{O}(n)$.

In a real-world SG scenario, where quick decision-making and energy optimization are critical, computational costs can have a substantial influence on the practicality of implementing numerous models at the same time. Models like SARIMAX and XGBoost, which provide excellent accuracy and integrate exogenous factors such as weather data, have a greater computational cost. This can be difficult in scenarios needing regular updates or retraining, especially during peak demand periods or when grid stability is critical. Models with simpler structures and shorter computation time, such as FBProphet and Holt–Winters, are more suited for real-time applications that require immediate forecasts to respond to short-term fluctuations in energy demand. Further, models like LSTM and Hybrid, while computationally expensive, can adapt to more complicated patterns over longer time horizons. Thus, the choice of model in a real-time SG scenario is determined by the trade-off between computational cost and the individual application's requirements, such as quick deployment or long-term prediction precision.

Both of these complexities for each model are also given in Table 11 for a better understanding.

Table 11. Time and space complexity of different models; lower complexity improves speed and efficiency, while more complexity provides better accuracy at the expense of additional resources.

Model	Time complexity	Space complexity
SARIMAX	$\mathcal{O}(n^2)$	$\mathcal{O}(n)$
Holt–Winters	$\mathcal{O}(n)$	$\mathcal{O}(n)$
LSTM	$\mathcal{O}(T \cdot n \cdot m)$	$\mathcal{O}(T \cdot n \cdot m)$
XGBoost	$\mathcal{O}(k \cdot d \cdot n \cdot \log n)$	$\mathcal{O}(k \cdot d \cdot n)$
FBProphet	$\mathcal{O}(n)$	$\mathcal{O}(n)$
Hybrid Model	$\mathcal{O}(m \cdot n)$	$\mathcal{O}(n)$

7. Parameter sensitivity and ablation study

7.1. Parameter sensitivity

A parameter sensitivity study was carried out to better understand the effect of various model hyperparameters on predicting accuracy. This entailed carefully changing the essential hyperparameters for each model and tracking changes in performance measures, such as MAE and RMSE.

- For SARIMAX, the AR order, MA order, and seasonal components were changed. As the AR and MA orders increased, the model improved its ability to capture long-term relationships. Still, it also caused overfitting on smaller training sets, resulting in a larger MAE.
- For FBProphet, the most important factors were the seasonalities (daily, weekly) and the changepoint before the scale. Adjusting the changepoint prior scale, which governs the model's ability to adapt to shifting trends, was critical to improving the model's performance. A larger changepoint prior scale enabled the model to detect more abrupt trend changes.
- For LSTM, the number of hidden units, learning rate, and sequence length were all modified. Increasing the number of hidden units enhanced the model's capacity to detect complicated temporal connections, resulting in longer training time and, in some cases, overfitting. A learning rate of 0.001 provided the optimal accuracy and training time.
- For the Holt–Winters exponential smoothing model, performance was susceptible to the smoothing parameters for level (α), trend (β^*), and seasonality (γ). A more excellent value of α allowed the model to respond more quickly to unexpected changes in the data at the price of capturing long-term patterns.
- For XGBoost, the maximum tree depth, number of estimators, and learning rate were all modified. A lower learning rate and a more significant number of estimators enhanced accuracy while increasing training time. A tree depth of *5* gave the optimal balance of accuracy and overfitting.
- For the hybrid model, Individual model weights were dynamically changed depending on recent forecasting errors, with initial weights set to equal levels. As the sliding window size increased, the recalibration became more consistent. However, a vast window size limited the model's capacity to respond to short-term variations in the data.

7.2. Ablation study

An ablation study was conducted to determine the contribution of various model components. This study eliminated specific characteristics or components, and the model's performance was re-evaluated. The results shed light on the relative relevance of different model components.

- For **SARIMAX**, we eliminated external factors, such as weather data. The model's performance worsened dramatically, with the MAE rising by about 15%, demonstrating power generation's high reliance on external meteorological conditions.
- In **FBProphet**, eliminating the holiday impacts and weekly seasonality components resulted in a 14% rise in MAPE highlighting the model's capacity to account for particular events, such as vacations and weekly trends critical for capturing fluctuations in power generation. When the holiday regressor was removed, Prophet struggled to catch some of the periodic changes caused by consumer behavior throughout holidays, resulting in more significant forecasting errors.
- For **LSTM**, removing the cyclical encoding of time (i.e., sine and cosine transformations for hour and day) resulted in a significant decline in performance (10% rise in MAPE), indicating that encoding time as a continuous cyclic feature is necessary for effective forecasting in this case.
- For **Holt–Winters**, removing the seasonality component increased the model's MAE by 12%, proving the importance of seasonal adjustments when predicting power generation with repeated cycles.
- For **XGBoost**, eliminating weather-related features like temperature and wind speed led to an increase in the MSE of around 12%. This demonstrates that external meteorological conditions are essential in determining power generation.

- In the **Hybrid Model**, omitting the dynamic recalibration process resulted in a performance reduction (increased MAE by 8%), emphasizing the necessity of adaptive weighting in maintaining accuracy under changing conditions.

8. Discussion and future work

This research demonstrates that integrating demand response systems with hyperlocal weather predictions in SGs may dramatically enhance power generation projections. Integrating granular meteorological data i.e., precipitation, temperature, relative humidity, apparent temperature, cloud cover, and wind speed, provided crucial insights into power generation predictions. Accurate weather prediction permitted more exact demand forecasting, allowing for improved resource allocation and energy distribution management.

We trained and evaluated five separate forecasting models before introducing a hybrid model that included the best of each three time series models. Our hybrid model's success was primarily due to its recalibration process, which enabled dynamic modifications to the weights allocated to separate models depending on real-time performance. The recalibration process guaranteed that the hybrid model could respond to new data, improving predicting accuracy across several situations. Recalibration is critical when weather conditions change abruptly because it allows the model to alter the contribution of each component (SARIMAX, Prophet, Holt–Winters) in real-time, improving overall performance.

One critical stage in feature engineering was transforming raw meteorological data into features capable of capturing temporal trends and correlations with energy usage. The hyper–local weather data was processed using lag terms, which allow the model to account for the delayed impacts of meteorological conditions on energy consumption. In addition, log transformations were utilized to stabilize variance, and cyclic encoding was used to capture better seasonal patterns (e.g., daily or weekly cycles).

Implementing the hybrid forecasting model in SGs can have a substantial environmental and economic impact, particularly in terms of improving energy efficiency and encouraging the use of renewable energy. More accurate STLF, as illustrated by our hybrid model, allows for more effective matching of energy demand to generation, lowering the requirement for fossil fuel-based backup power. This immediately leads to fewer carbon emissions and energy waste, since improved forecasting reduces energy overproduction and prevents excessive restricting of RESs. Economically, our model's correct forecasting provides significant cost savings to grid operators. By reducing forecast errors, the model minimizes the requirement for costly reserve power and the financial penalties associated with energy imbalances (Ahmed & Khalid, 2019). Improved forecasts can also lead to more effective energy trading and scheduling, which reduces SG operational costs.

Despite the encouraging outcomes, certain restrictions appeared. The individual models struggled to capture non-linear patterns, different seasonalities, and sudden changes in meteorological conditions. These problems highlight the complexities of estimating electricity generation in changing contexts. Although the hybrid technique helped to address some of these shortcomings, further work is needed to increase the model's flexibility and adaptability in dealing with a wide range of forecasting scenarios. The research also faces limitations in terms of data quality and availability. The lack of comprehensive, publicly available datasets limited the capacity for in-depth analysis across extended periods. In contrast, time series data from SG batteries offered sufficient variables for STLF, however, the availability of just one month's data limited efforts to expand the model's applicability to long-term load forecasting (LTLF). The short data span hindered the hybrid model's capacity to capture more complicated temporal patterns required for reliable long-term forecasts. Training the hybrid model on a more diversified dataset will allow it to expand its prediction powers from STLF to LTLF with minor methodological changes. Expanding the temporal coverage and including more granular weather and energy consumption data would strengthen the model's ability to anticipate for more extended periods.

Moving forward, we also want to investigate further DL models and ensemble approaches to improve forecast accuracy. Transformers, recurrent neural networks (RNNs), and LSTM networks are ideal for time series forecasting because they can capture complicated non-linear interactions. Integrating these DL models into the hybrid framework can significantly enhance short- and long-term predictions. Furthermore, ensemble strategies that integrate the outputs of numerous DL models may improve performance, especially in settings with highly variable or non-linear energy demand patterns. While hybrid models and DL techniques achieve incredible accuracy, they are sometimes viewed as black-box models, making it difficult for stakeholders to comprehend the underlying reasoning. Incorporating Explainable AI (XAI) approaches into the hybrid model is critical for obtaining user confidence. XAI may give insights into the contributions of numerous elements (weather conditions and historical energy demand) to final forecasts, assisting energy stakeholders in understanding the factors that influence projections. This can help the model gain acceptability, especially in regulatory or operational situations where transparency is essential. Nonetheless, Federated learning (FL) also represents an attractive avenue for future study, mainly in SGs where data privacy and security are critical.

On the implementation side, the main focus is improving user engagement with the forecasting system. Developing real-time, interactive dashboards employing modern data visualization frameworks will enhance the user experience and enable faster decision-making. Optimizing the model's training pipelines and using computationally efficient methods would minimize response times, allowing users to produce near-instantaneous forecasts instead of waiting 180–240 seconds. By reducing the interface between users and the model, we can ensure that projections are supplied more quickly and efficiently, boosting overall operational performance.

Finally, lowering computational overhead is critical to ensuring the forecasting system can be used in real-time, large-scale scenarios. Investigating computationally economic models that can nevertheless offer accurate forecasts will be crucial for the practical use of this hybrid forecasting method. This reduces forecasting time and makes the system more flexible to various use cases, ranging from small-scale energy grids to more extensive regional networks.

9. Conclusion

This study is intensely focused on short-term load forecasting, utilizing the improved capabilities of smart grids to improve the precision and dependability of upcoming energy demand and supply projections. The thorough analysis sheds light on the considerable improvement in power generation efficiency obtained in SGs through the novel combination of demand response mechanisms and hyperlocal weather predictions. Among the five individual models, i.e., SARIMAX, Prophet, Holt–Winters, XGBoost, and LSTM, SARIMAX outperformed the rest with an MAE of 3.54 and an R^2 score of 0.97 for the 24-hour forecast. Our research introduced a hyperlocal model that combines the strengths of SARIMAX, Prophet, and Holt–Winters in an ensemble approach. The hybrid model provides quicker training times because of its benefits in parallelization and smaller model components. Furthermore, the hybrid model includes a dynamic recalibration system that modifies the weights of each component model in real-time, increasing flexibility and predicting accuracy depending on current data. However, the model's accuracy relies heavily on the quality and availability of input data, and its suitability for long-term forecasting is limited. The hybrid model's complexity demands substantial computational resources, and integrating multiple models can make interpretability challenging. Future studies will focus on integrating larger datasets over more extended periods and adding variables like renewable energy statistics and economic indicators to improve the model's resilience and accuracy. Advanced deep learning models, transformers, and continuous learning approaches will be investigated to adapt to changing data patterns over time. Furthermore, Federated Learning will enable decentralized model training while protecting data privacy. Explainable AI will be investigated to increase model interpretability, providing stakeholders with insights into how specific attributes impact forecasts.

Notes

1. P. Patil, Time Series Data of Battery Energy Storage System (2023). https://ieee-dataport.org/documents/time-series-data-battery-energy-storage-system.
2. Open-Meteo - Historical weather api. https://open-meteo.com/en/docs/historical-weather-api.

Acknowledgements

The authors would like to acknowledge the support of Prince Sultan University for paying the Article Processing Charges of this publication.

Ethics approval and consent to participate

Not applicable.

Authors contributions

Conceptualization: F.S. and H.A.K.; Data curation: F.S. and H.S.A.; Formal analysis: F.S. and H.S.A.; Funding acquisition: H.A.K., H.F. and M.M.N.; Investigation: F.S. and H.A.K.; Methodology: F.S., H.A.K. and H.S.A.; Project administration: H.A.K. and M.M.N.; Resources: F.S., H.A.K. and H.F.; Software: H.A.K.; Supervision: H.A.K.; Validation: H.F. and M.M.N.; Visualization: H.A.K. and H.S.A.; Writing–original draft: F.S., H.A.K. and H.S.A.; Writing–review and editing: H.A.K., H.F. and M.M.N. All authors have read and approved the final version of the manuscript.

Consent for publication

All authors have reviewed and approved the manuscript.

Disclosure statement

No potential competing interest was reported by the author(s).

Funding

This article is derived from a research grant funded by the Research, Development, and Innovation Authority (RDIA)-Kingdom of Saudi Arabia-with grant number (13292-psu-2023-PSNU-R-3-1-EF-).

About the authors

Faraz Shaikh received his Master's degree in Computational Science and Engineering from the National University of Sciences and Technology (NUST), Islamabad, Pakistan. He is currently pursuing his PhD in the Department of Engineering at the University of Perugia, Italy. His doctoral research focuses on advancing artificial intelligence techniques for cloud-native and edge computing environments, with particular emphasis on autoscaling, resource orchestration, and distributed intelligence in 6G networks. In addition to his doctoral work, Faraz has contributed to a wide range of projects in artificial intelligence, machine learning, and deep learning. His interdisciplinary expertise bridges theoretical modeling with applied research in domains such as smart grids, cloud computing, and next-generation networking. He has also collaborated on projects in scientific machine learning, robustness in AI systems, and reinforcement learning for complex environments. With a strong background in both academic research and practical implementations, he is committed to developing intelligent, adaptive, and energy-efficient solutions for emerging computing paradigms.

Hasan Ali Khattak is a Senior Lecturer at Western Sydney University, Australia, and an Associate Professor of Computer Science at the School of Electrical Engineering and Computer Science at the National University of Sciences and Technology (NUST), Islamabad, Pakistan. He earned his PhD in Electrical and Computer Engineering from Politecnico di Bari, Bari, Italy, in April 2015. With over 12 years of teaching experience at various universities in Oman, Australia, Italy, and Pakistan, he has held numerous roles, including course coordinator, theme leader, and industry liaison focal person. He has contributed to various committees responsible for accreditation by the Washington Accord, the Australian Computer Society, and the Pakistan Higher Education Commission for both graduate and undergraduate programmes. He has supervised more than four dozen Master's students, most of whom are pursuing doctoral studies in international universities. Having completed several funded projects and supervised many PhD graduates, his current research interests focus on future Internet architectures such as the Web of Things, as well as leveraging data sciences and social engineering for developing smarter cities. Hasan Ali Khattak can be contacted on hasan@khattak.info or https://hasan.khattak.info

Hasan Sohaib Alavi is a Senior Research and Development Engineer (AI) at Beyond Engineering NL, Netherlands, and Co-Founder of SnackAI, an AI education platform focused on practical, human-centered artificial intelligence. He holds a Master of Science in Computational Science and Engineering from the National University of Sciences and Technology (NUST), Pakistan. His research expertise spans artificial intelligence applications in healthcare, medical image analysis, biomechanics, and systems thinking approaches. Alavi has made significant contributions to medical AI, particularly in developing device-agnostic models for retinal OCT segmentation, confidence-aware deep learning frameworks, and physics-informed neural networks for biomechanical analysis. His work at OIRRC (Ocular Imaging Research and Reading Center, commercial front of Sepah lab, School of Medicine, Stanford) involved developing

AI-assisted workflows for ophthalmological diagnostics and leading organizational transformation initiatives. As an Associate Researcher at NUST's Biomedical Engineering Research Group, Alavi advanced research in human biomechanics, motion capture technologies, and assistive device development. His interdisciplinary approach combines technical expertise in machine learning, deep learning, and data analytics with practical applications in healthcare technology and business innovation. Alavi has contributed to multiple peer-reviewed publications and is currently advancing research in domain generalization for healthcare imaging, multimodal neural network functionality, AI in healthcare, and design thinking methodologies for business innovation. His research philosophy centers on research-to-commercialization-and-impact (R2CI), bridging the gap between academic research and real-world impact. He has extensive teaching experience, having instructed over 35 engineering courses and mentored numerous students and professionals in AI and machine learning applications.

Haleem Farman is a distinguished researcher at Prince Sultan University, Riyadh, where he is actively involved in various R&D activities within the Smart Systems Engineering Research Lab. Haleem specializes in the Internet of Things, Privacy Preservation and Intrusion Detection Systems, Adhoc Networks, Smart Cities, Smart Education, and Artificial Intelligence. Haleem has played key roles in numerous research-funded projects, serving as Principal Investigator (PI), Co-Principal Investigator (Co-PI), and team member. His work has been supported by esteemed donor agencies, including the British Council, the Research and Development Initiative Authority of Saudi Arabia, Prince Sultan University, and the Government of Pakistan. His projects primarily focus on advancements in the Internet of Things and Artificial Intelligence. His extensive experience in teaching and supervision is a testament to his dedication to education and research. Moreover, Haleem mentored numerous undergraduate and postgraduate students, guiding them in their research activities and fostering a passion for academic excellence. Haleem's extensive publication record, comprising over 55 articles in high-impact journals, conferences, and book chapters, demonstrates his commitment to knowledge dissemination and contribution to the academic community. His active membership in professional organizations such as IEEE (Senior Member) and IEEE Young Professionals further underscores his dedication to the field and ongoing engagement with the professional community. Additionally, Haleem serves as the Vice-Chair of the IEEE Smart Cities Awards and Recognition Committee, reflecting my leadership and commitment to advancing smart city technologies. Moreover, Haleem also serves as the IEEE VTS Young Professional Ambassador for 2025-2026.

Dr. Moustafa M. Nasralla (Senior Member, IEEE) received a BSc (Hons) in Electrical Engineering from Hashemite University, Jordan, in 2010, an MSc in Networking and Data Communications from Kingston University, London, U.K., in 2011, and a PhD from the Faculty of Science, Engineering and Computing (SEC), Kingston University. He is currently an Associate Professor and Chairman of the Department of Communications and Networks Engineering at Prince Sultan University (PSU), Riyadh, Saudi Arabia, where he also leads the Smart Systems Engineering Laboratory (SSEL). He is an alumni member of the Wireless Multimedia and Networking (WMN) Research Group at Kingston University. Dr. Nasralla has served as an active reviewer and has received several distinguished reviewer awards from reputable journals such as IEEE Transactions on Wireless Communications, IEEE Transactions on Multimedia, IEEE Transactions on Vehicular Technology, Wireless Communications (Elsevier), and Computer Networks (Elsevier). His research contributions in networks and data communications are evidenced by his publications in ISI Thomson JCR journals. He has led several national and international projects, including towards smart cities using IoT and AI in Saudi Arabia, Intelli-Student for the British Council, 5G-enabled Smart City Development in Saudi Arabia, U.K. Home Office, and EU FP7 CONCERTO. Currently, he serves as a Guest Editor for the Alexandria Engineering Journal (Elsevier), the International Journal of Distributed Sensor Networks (SAGE), and the Journal of Communications and Networks (Frontiers). He is also an organizer for the International Conference on Sustainability: Developments and Innovations and the 5G-Enabled Smart Cities workshop at the IEEE International Conference on Smart Cities. Additionally, he is a Senior Member of IEEE Young Professionals, IEEE ComSoc, and the Association for Computing Machinery (ACM). Moreover, he serves as the Chair of the IEEE Smart Cities Awards and Recognition Committee, reflecting his leadership and commitment to advancing smart city technologies. He has published over 80 articles in high-impact journals and reputable conferences. His research interests include the latest wireless communication systems (e.g., 6G, 5G, LTE-A, and LTE wireless networks), wireless sensor networks, network security, the Internet of Things (IoT), machine learning, radio resource allocation, telemedicine and video compression, and multimedia communications. He is a Fellow of the Higher Education Academy (FHEA).

ORCID

Faraz Shaikh http://orcid.org/0009-0005-7815-8283
Hasan Ali Khattak http://orcid.org/0000-0002-8198-9265
Hasan Sohaib Alavi http://orcid.org/0000-0002-5051-9703
Haleem Farman http://orcid.org/0000-0003-2344-1522
Moustafa M. Nasralla http://orcid.org/0000-0002-6511-1460

Availability of data and materials

Data will be provided upon reasonable request to Faraz Shaikh at faraz@dottorandi.unipg.it

References

Adkins, K. A., Becker, W., Ayyalasomayajula, S., Lavenstein, S., Vlachou, K., Miller, D., Compere, M., Muthu Krishnan, A., & Macchiarella, N. (2023). Hyper–local weather predictions with the enhanced general urban area microclimate predictions tool. *Drones*, *7*(7), 428. https://doi.org/10.3390/drones7070428

Adnan, M., Ghadi, Y., Ahmed, I., & Ali, M. (2023). Transmission network planning in super smart grids: A survey. *IEEE Access*, *11*, 77163–77227. https://doi.org/10.1109/ACCESS.2023.3296152

Ahmed, R. A., Abdelraouf, M., Elsaid, S. A., ElAffendi, M., El-Latif, A. A. A., Shaalan, A. A., & Ateya, A. A. (2024). Internet of Things-Based Robust Green Smart Grid. *Computers*, *13*(7), 169 https://doi.org/10.3390/computers13070169

Ahmed, A., & Khalid, M. (2019). A review on the selected applications of forecasting models in renewable power systems. *Renewable & Sustainable Energy Reviews*, *100*, 9–21. https://doi.org/10.1016/j.rser.2018.09.046

Almazrouee, A. I., Almeshal, A. M., Almutairi, A. S., Alenezi, M. R., & Alhajeri, S. N. (2020). Long-term forecasting of electrical loads in Kuwait using prophet and holt–winters models. *Applied Sciences*, *10*(16), 5627. https://doi.org/10.3390/app10165627

Amin, W., Huang, Q., Li, J., Khan, A. A., Subramaniam, U., & Selvam, S. (2025). A secure energy management model for Peer-to-Peer smart grids with user-centric constraints. *Internet of Things*, 101678. https://doi.org/10.1016/j.iot.2025.101678.

Arumugham, V., Ghanimi, H. M. A., Pustokhin, D. A., Pustokhina, I. V., Ponnam, V. S., Alharbi, M., Krishnamoorthy, P., & Sengan, S. (2023). An artificial-intelligence-based renewable energy prediction program for demand-side management in smart grids. *Sustainability*, *15*(6), 5453. https://doi.org/10.3390/su15065453

Bakare, M. S., Abdulkarim, A., Zeeshan, M., & Shuaibu, A. N. (2023). A comprehensive overview on demand side energy management towards smart grids: Challenges, solutions, and future direction. *Energy Informatics*, *6*(1), 1–59. https://doi.org/10.1186/s42162-023-00262-7

Balážová, R., Hlinka, J., Belbachir, A., & Svoboda, J. (2024). *Hyperlocal weather information for drone operations* [Paper presentation]. In 2024 New Trends in Civil Aviation (NTCA) (pp. 67–73). IEEE. https://doi.org/10.23919/NTCA60572.2024.10517813

Carrera, B., & Kim, K. (2020). Comparison analysis of machine learning techniques for photovoltaic prediction using weather sensor data. *Sensors*, *20*(11), 3129. https://doi.org/10.3390/s20113129

Carreras, B. A., Colet, P., Reynolds-Barredo, J. M., & Gomila, D. (2021). Assessing blackout risk with high penetration of variable renewable energies. *IEEE Access*, *9*, 132663–132674. https://doi.org/10.1109/ACCESS.2021.3114121

Das, D., & Chakrabarti, S. (2021). Forecasting non-linear WPI of manufacture of chemicals and chemical products in India: An MLP approach. *International Journal of Advanced Technology & Engineering Exploration*, *8*(82), 1193–1207. https://doi.org/10.19101/IJATEE.2021.874407

Dudek, G., Smyl, S., & Pełka, P. (2022). Recurrent neural networks for forecasting time series with multiple seasonality: A comparative study. In: Valenzuela, O., Rojas, F., Herrera, L.J., Pomares, H., Rojas, I. (eds) Theory and Applications of Time Series Analysis. ITISE. Contributions to Statistics. Springer, Cham; 2022. pp. 171–185. https://doi.org/10.1007/978-3-031-40209-8_12

Elshewey, A. M., Shams, M. Y., Elhady, A. M., Shohieb, S. M., Abdelhamid, A. A., Ibrahim, A., & Tarek, Z. (2022). A novel Wd-Sarimax model for temperature forecasting using daily Delhi climate dataset. *Sustainability*, *15*(1), 757. https://doi.org/10.3390/su15010757

FitzPatrick, G. J., & Wollman, D. A. (2010). *Nist interoperability framework and action plans* [Paper presentation]. IEEE PES General Meeting, pp. 1–4.

Gowtham, N., Prema, V., Elmorshedy, M. F., Bhaskar, M. S., & Almakhles, D. J. (2023). A power aware long short-term memory with deep brief network based microgrid framework to maintain sustainable energy management and load balancing. *Distributed Generation & Alternative Energy Journal*, *39*(01), 1–26. https://doi.org/10.13052/dgaej2156-3306.3911

He, Z., Lin, R., Wu, B., Zhao, X., & Zou, H. (2023). Pre-attention mechanism and convolutional neural network based multivariate load prediction for demand response. *Energies*, *16*(8), 3446. https://doi.org/10.3390/en16083446

Ibrahim, B., Rabelo, L., Gutierrez-Franco, E., & Clavijo-Buritica, N. (2022). Machine learning for short-term load forecasting in smart grids. *Energies*, *15*(21), 8079. https://doi.org/10.3390/en15218079

Jamii, J., Mansouri, M., Trabelsi, M., Mimouni, M. F., & Shatanawi, W. (2022). Effective artificial neural network-based wind power generation and load demand forecasting for optimum energy management. *Frontiers in Energy Research*, *10*, 898413. https://doi.org/10.3389/fenrg.2022.898413

Jamil, F. (2018). Electricity theft among residential consumers in Rawalpindi and Islamabad. *Energy Policy*, *123*, 147–154. https://doi.org/10.1016/j.enpol.2018.04.023

Krishna, V. B., Wadman, W. S., & Kim, Y. (2018). Nowcasting: Accurate and precise short-term wind power prediction using hyperlocal wind forecasts. In *Proceedings of the Ninth International Conference on Future Energy Systems* (pp 63–74).

Kumari, S., Kumar, N., & Rana, P. S. (2022). A big data approach for demand response management in smart grid using the prophet model. *Electronics*, *11*(14), 2179. https://doi.org/10.3390/electronics11142179
Li, P., & Sharma, A. (2024). Hyper–local temperature prediction using detailed urban climate informatics. *Journal of Advances in Modeling Earth Systems*, *16*(3), e2023MS003943. https://doi.org/10.1029/2023MS003943
Livieris, I. E., Stavroyiannis, S., Iliadis, L., & Pintelas, P. (2021). Smoothing and stationarity enforcement framework for deep learning time-series forecasting. *Neural Computing & Applications*, *33*(20), 14021–14035. https://doi.org/10.1007/s00521-021-06043-1
Łoś, H., Sousa Mendes, G., Cordeiro, D., Grosso, N., Costa, H., Benevides, P., & Caetano, M. (2021). Evaluation of xgboost and lgbm performance in tree species classification with sentinel-2 data. In *2021 IEEE International Geoscience and Remote Sensing Symposium IGARSS* (pp 5803–5806). IEEE.
Manninen, H., Lippus, M., & Rute, G. (2024). Dynamic line rating using hyper–local weather predictions: A machine learning approach. arXiv preprint arXiv:2405.12319
Pasari, S., & Shah, A. (2020). Time series auto-regressive integrated moving average model for renewable energy forecasting. In *Enhancing Future Skills and Entrepreneurship: 3rd Indo-German Conference on Sustainability in Engineering* (pp 71–77). Springer International Publishing Cham.
Patrizi, N., LaTouf, S. K., Tsiropoulou, E. E., & Papavassiliou, S. (2022). Prosumer-centric self-sustained smart grid systems. *IEEE Systems Journal*, *16*(4), 6042–6053. https://doi.org/10.1109/JSYST.2022.3156877
Rajagopalan, A., Swaminathan, D., Alharbi, M., Sengan, S., Montoya, O. D., El-Shafai, W., Fouda, M. M., & Aly, M. H. (2022). Modernized Planning of Smart Grid Based on Distributed Power Generations and Energy Storage Systems Using Soft Computing Methods. *Energies*, *15*(23), 8889. https://doi.org/10.3390/en15238889
Salazar, E. J., Jurado, M., & Samper, M. E. (2023). Reinforcement learning-based pricing and incentive strategy for demand response in smart grids. *Energies*, *16*(3), 1466. https://doi.org/10.3390/en16031466
Sathyaraj, J., & Sankardoss, V. (2024). A novel analysis of random forest regression model for wind speed forecasting. *Cogent Engineering*, *11*(1), 2434617. https://doi.org/10.1080/23311916.2024.2434617
Shaikh, F., & Khattak, H. A. (2024, October). Hybrid Forecasting Model for Smart Grid Using Exogenous Variables. In 2024 International Conference on Emerging Trends in Smart Technologies (ICETST) (pp. 1–6). https://doi.org/10.1109/ICETST62952.2024.10737930, IEEE.
Shannon, B. (2019). Big o notation – Why it matters (and why it doesn't). Accessed: 2024-09-05.
Tarmanini, C., Sarma, N., Gezegin, C., & Ozgonenel, O. (2023). Short term load forecasting based on ARIMA and ANN approaches. *Energy Reports*, *9*, 550–557. https://doi.org/10.1016/j.egyr.2023.01.060
Ullah, K., Khan, T. A., Hafeez, G., Khan, I., Murawwat, S., Alamri, B., Ali, F., Ali, S., & Khan, S. (2022). Demand side management strategy for multi-objective day-ahead scheduling considering wind energy in smart grid. *Energies*, *15*(19), 6900. https://doi.org/10.3390/en15196900
Venter, Z. S., Brousse, O., Esau, I., & Meier, F. (2020). Hyperlocal mapping of urban air temperature using remote sensing and crowdsourced weather data. *Remote Sensing of Environment*, *242*, 111791. https://doi.org/10.1016/j.rse.2020.111791
Wang, J. C. (2019). Analysis of energy use intensity and greenhouse gas emissions for universities in Taiwan. *Journal of Cleaner Production*, *241*, 118363. https://doi.org/10.1016/j.jclepro.2019.118363
Wang, Y., Qi, Y., Li, J., Huan, L., Li, Y., Xie, B., & Wang, Y. (2023). The wind and photovoltaic power forecasting method based on digital twins. *Applied Sciences*, *13*(14), 8374. https://doi.org/10.3390/app13148374
World Bank. (2020). Pakistan: Reforms for a brighter future: Policy note 5 – Achieving sustainable energy.
Xia, M., Shao, H., Ma, X., & de Silva, C. W. (2021). A stacked gru-rnn-based approach for predicting renewable energy and electricity load for smart grid operation. *IEEE Transactions on Industrial Informatics*, *17*(10), 7050–7059. https://doi.org/10.1109/TII.2021.3056867
Zaidan, M. A., Motlagh, N. H., Zakeri, B., Petäjä, T., Kulmala, M., & Tarkoma, S. (2024). Irmaset: Intelligent weather forecaster system for hyper–local renewable energies. *IEEE Consumer Electronics Magazine*, *13*(5), 61–74. https://doi.org/10.1109/MCE.2024.3382438
Zhang, H., Zhang, M., Yi, R., Liu, Y., Han Wen, Q., & Meng, X. (2024). Growing importance of micro-meteorology in the new power system: Review, analysis and case study. *Energies*, *17*(6), 1365. https://doi.org/10.3390/en17061365